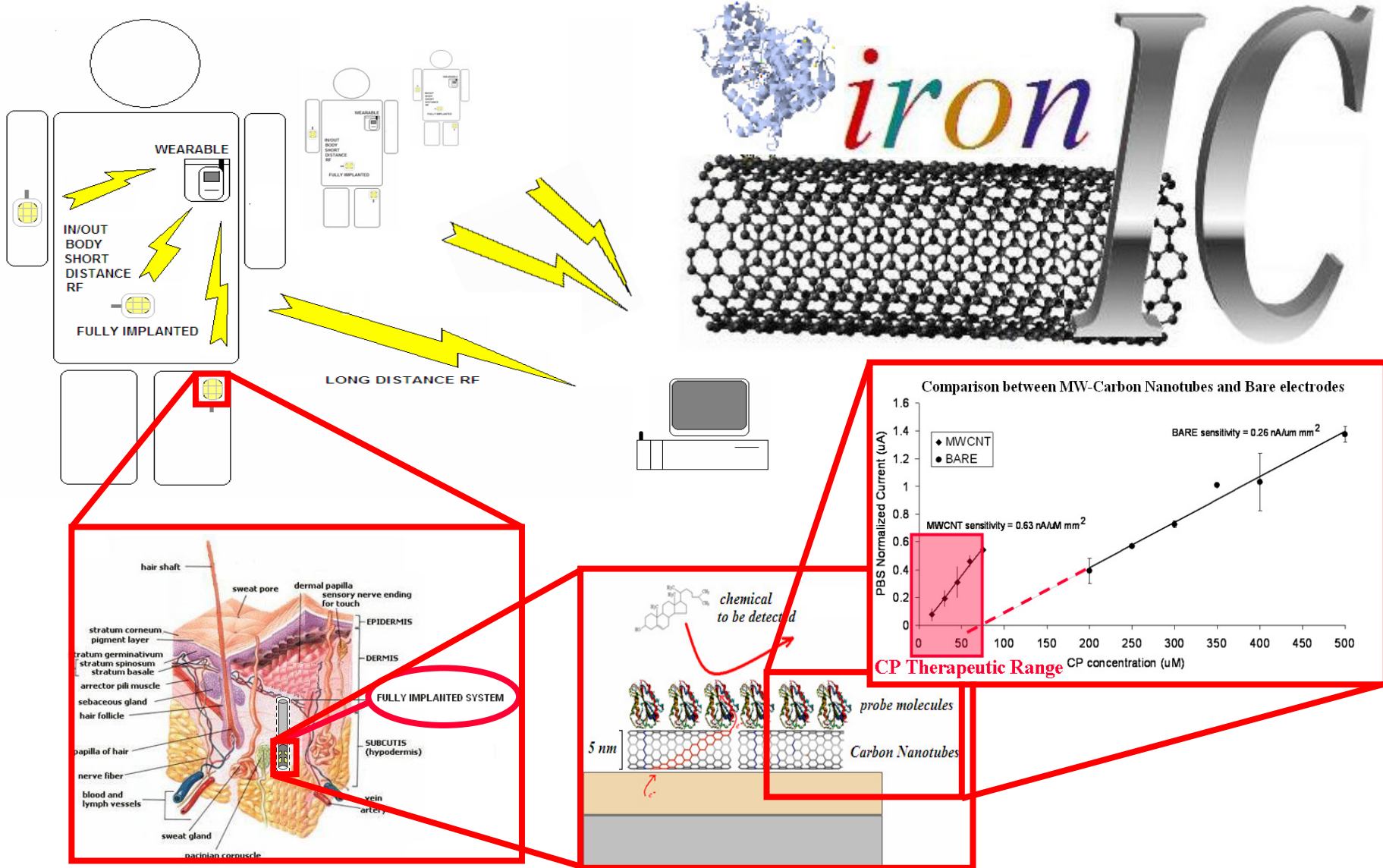


Developing Subcutaneous Fully-implanted Biochips for Remote Monitoring of Human Metabolism

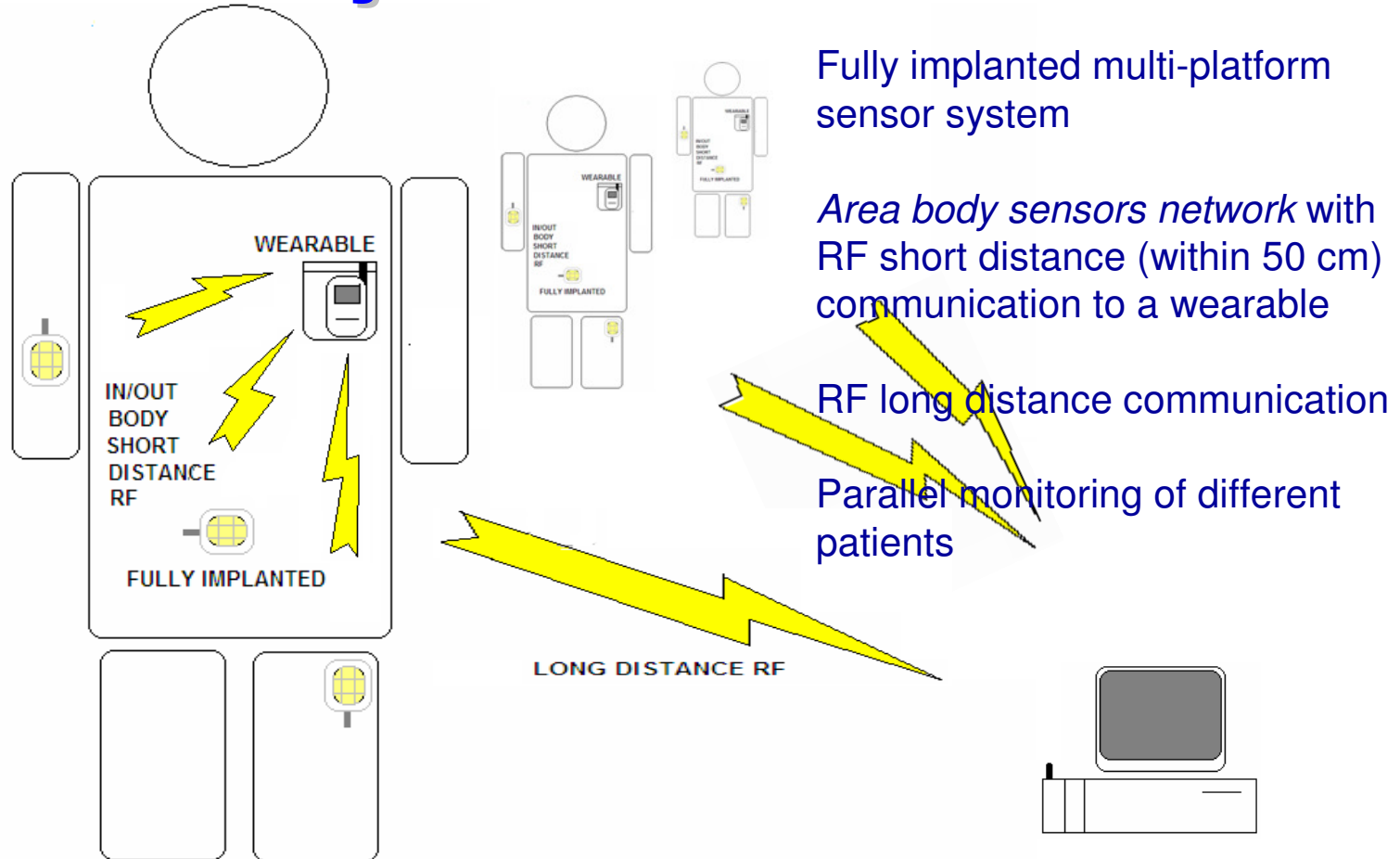


NT project Implantable-IRONIC



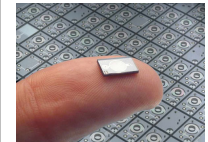
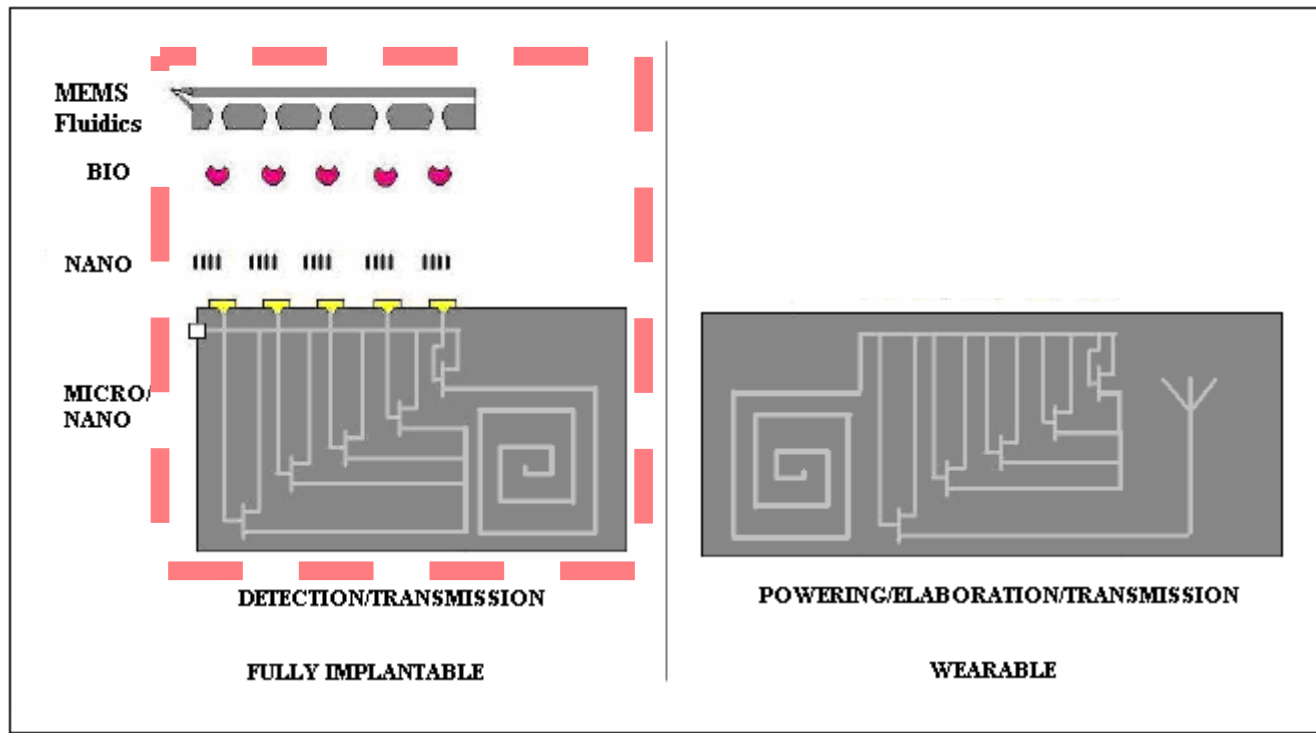


Project Main Goals



Design implantable/wearable systems for continuous monitoring of human metabolism

System Level Integration



Micro/Nano/Bio technology integration

State-of-the-Art

A. Menarini Diagnostics, Florence



- In/Out tubing
- Almost only for Diabetes
- Almost only for Glucose

GlucoDay® and GlucoMenDay® consist of a micro-pump and a biosensor coupled with a micro-dialysis system

New sub-cutaneous system

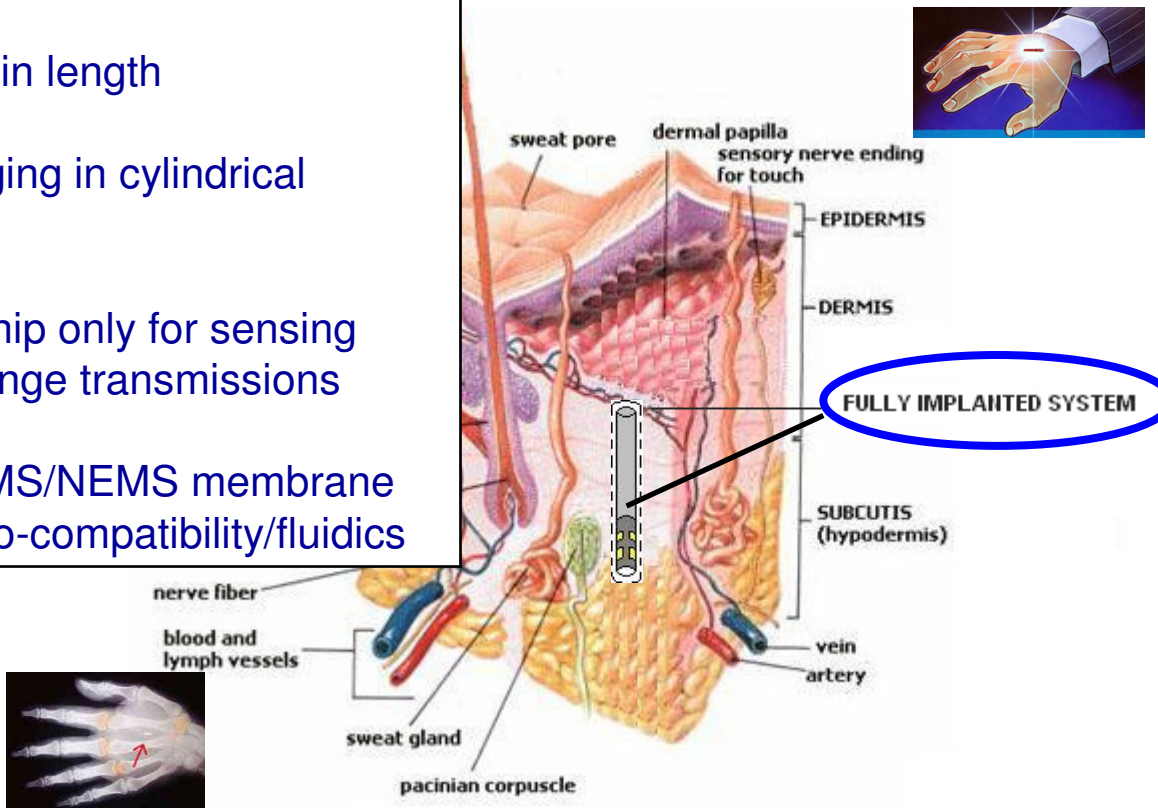
Cylinder: 1-2 mm in diameter

Below 2 cm in length

Chip packaging in cylindrical shape

Implanted chip only for sensing and short range transmissions

Porous MEMS/NEMS membrane to ensure bio-compatibility/fluidics



Fully implanted system with fluidics, sensors, electronics, antenna, data processing and transmission

Innovative aspects

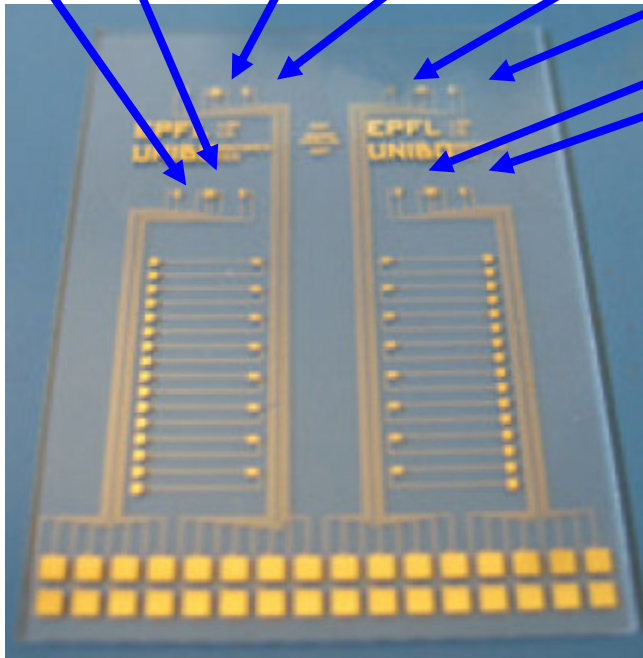
- Multi-panel metabolite detection
 - New array-based biosensors
- Ultra-low power data processing and transmission electronics
 - Power transmission
- Reliable distributed data processing
 - In situ* and off line

Direct benefits include lower cost and more accurate health monitoring and support for personal nutrition studies

Sensor array architecture

Probe enzymes

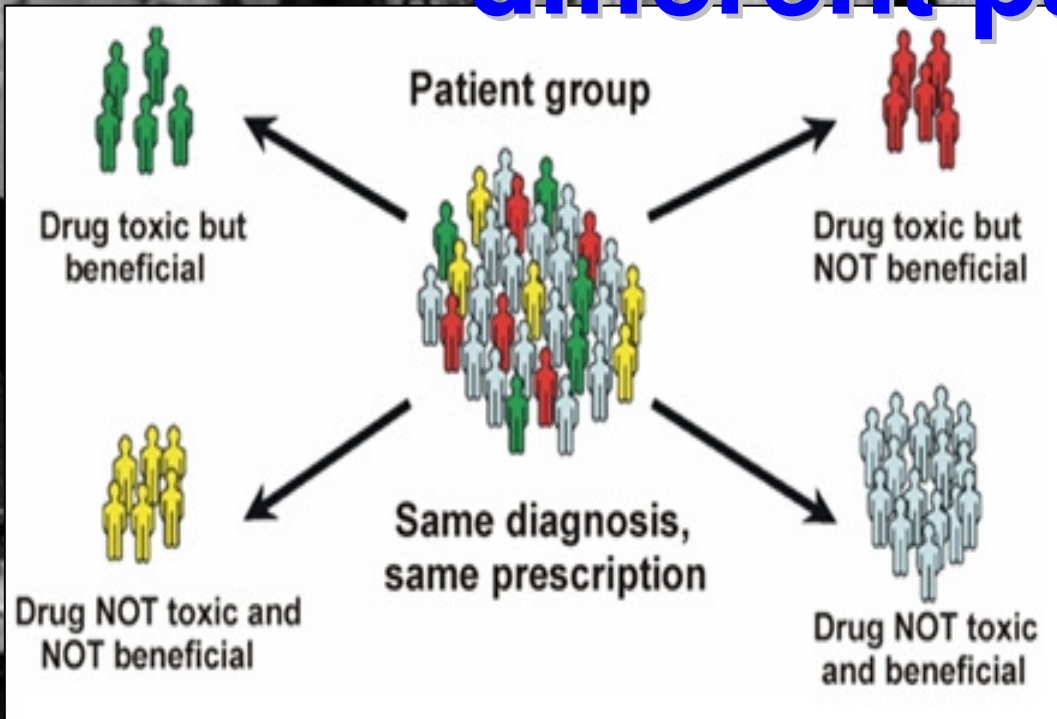
ATP-ase	Lactate oxidase	Glucose oxidase	Lipoxygenase
P450 11A1	P450 5A1	P450 4A11	Cholesterol oxidase



- Glucose
- Lactate
- Cholesterol
- Triglycerides
- Drugs

Different enzymes sense different target metabolites

Different outcomes for different patients



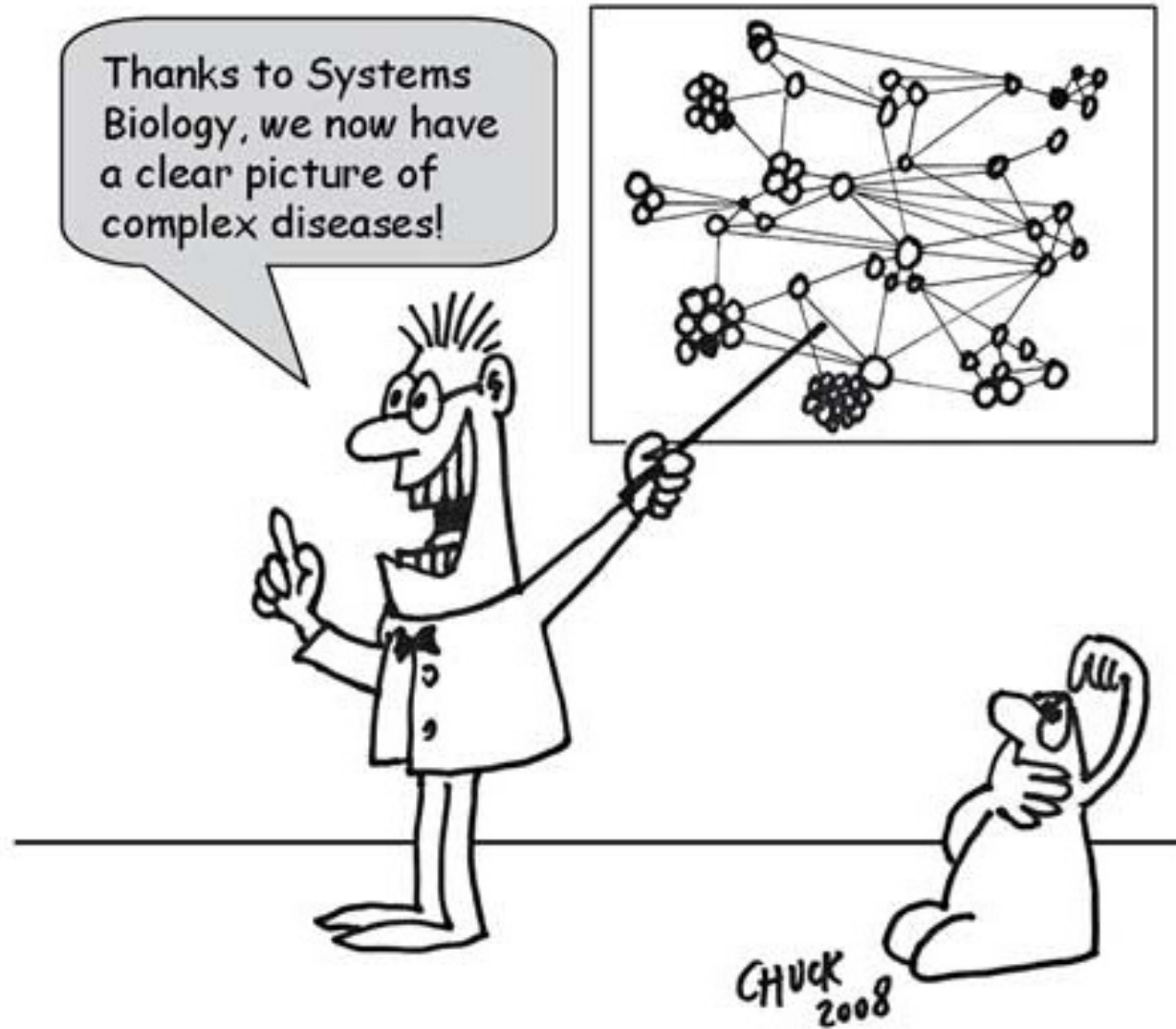
Therapeutic area	Rate of efficacy with standard drug treatment
Cancer (all types)	25%
Alzheimer's disease	30%
Incontinence	40%
Hepatitis C	47%
Osteoporosis	48%
Rheumatoid arthritis	50%
Migraine (prophylaxis)	50%
Migraine (acute)	52%
Diabetes	57%
Asthma	60%
Cardiac arrhythmias	60%
Schizophrenia	60%
Depression	62%

For depression, the data apply specifically to the drug class known as selective serotonin reuptake inhibitors.

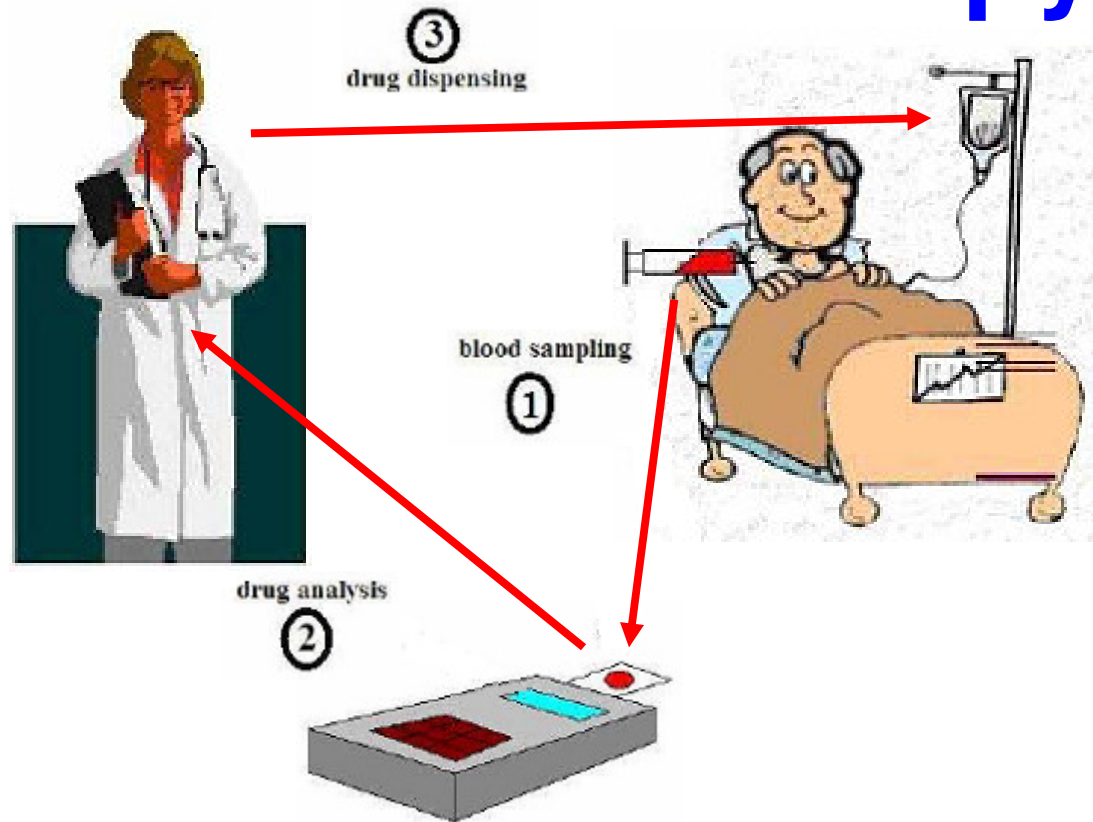
Source: Brian B. Spear, Margo Heath-Chiozzi, and Jeffrey Huff, "Clinical Application of Pharmacogenetics," *Trends in Molecular Medicine* (May 2001).



System Biology is not enough



Point-of-Care in Personalized Therapy



The Development of Monitoring Point-of-Care Devices is a key-factor for succeeding in Personalized therapy



The Motivation

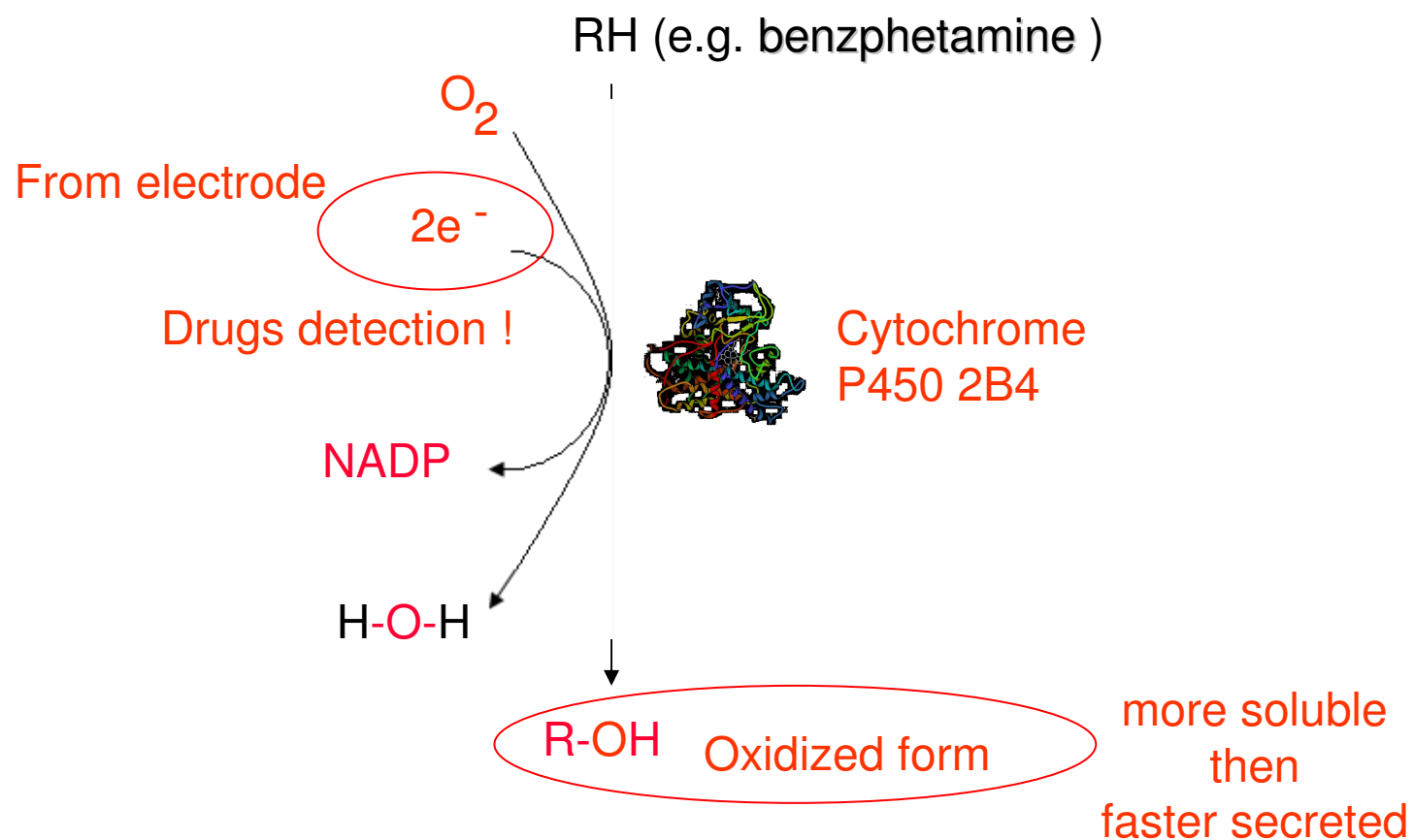


- 100.000 \$ (machinery)
- 1.000 \$ the single μ -array

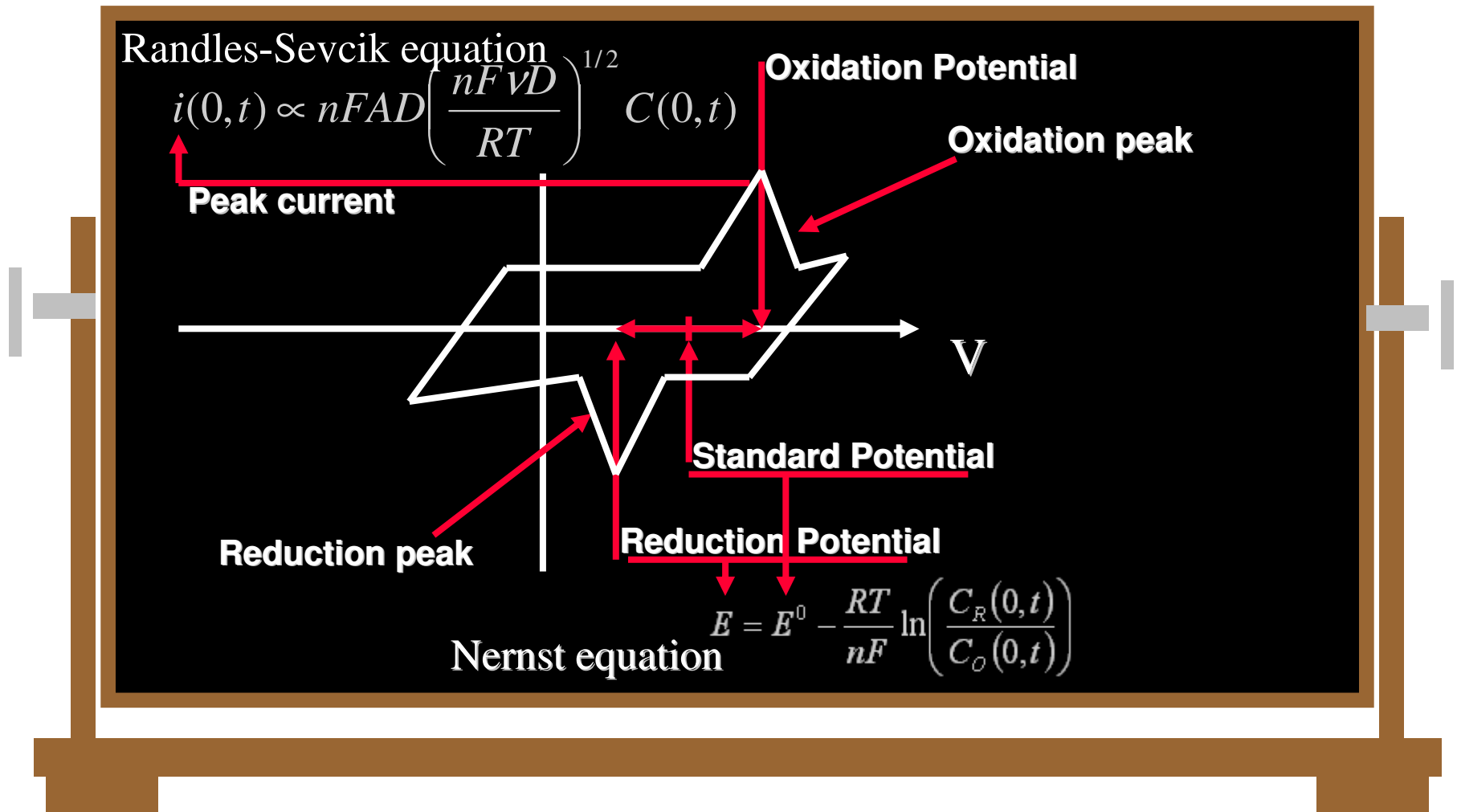


- 50 \$ (machinery)
- 0.05 \$ the single strip

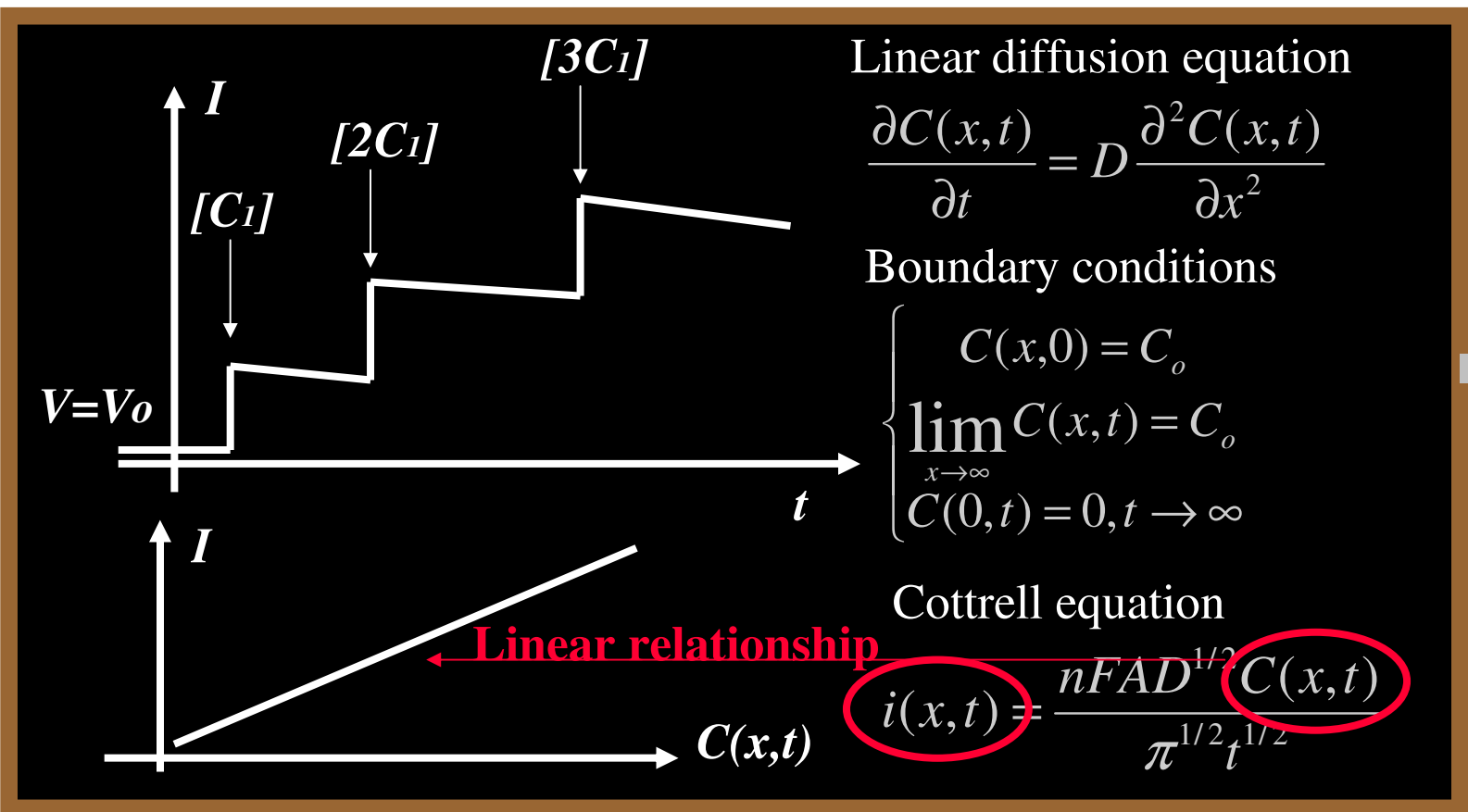
P450 for Drugs Monitoring



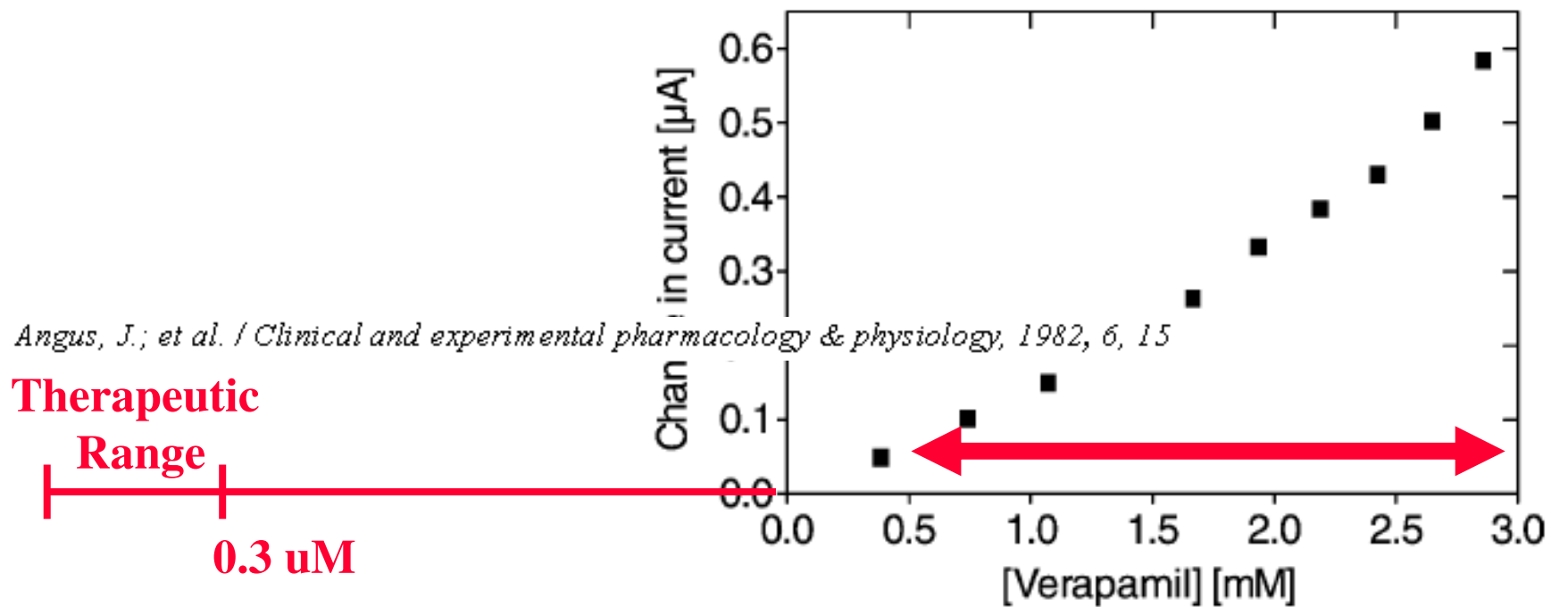
Drugs detection from Voltammetry



Drugs detection from Amperometry



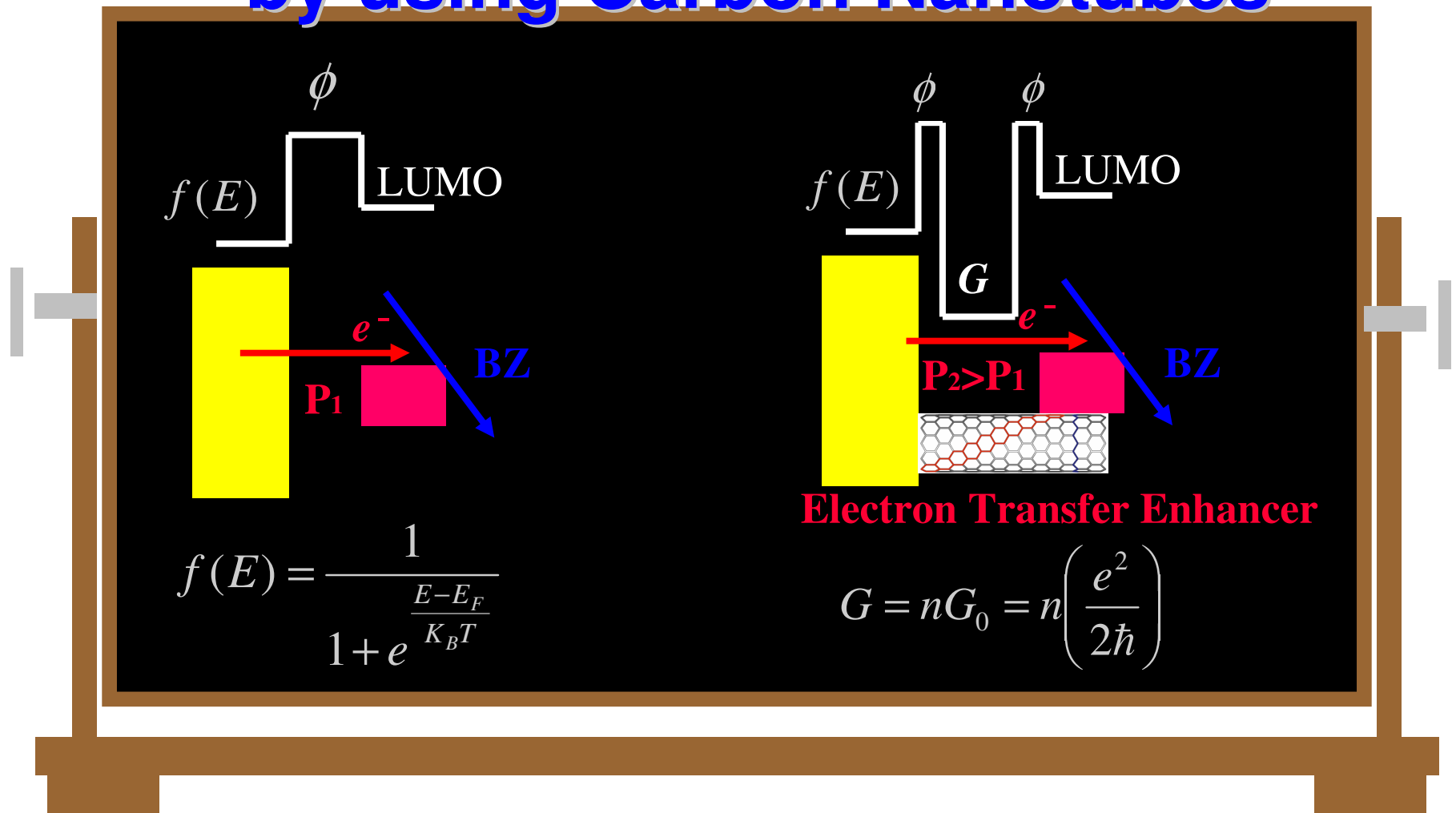
Problems on Detection Limits



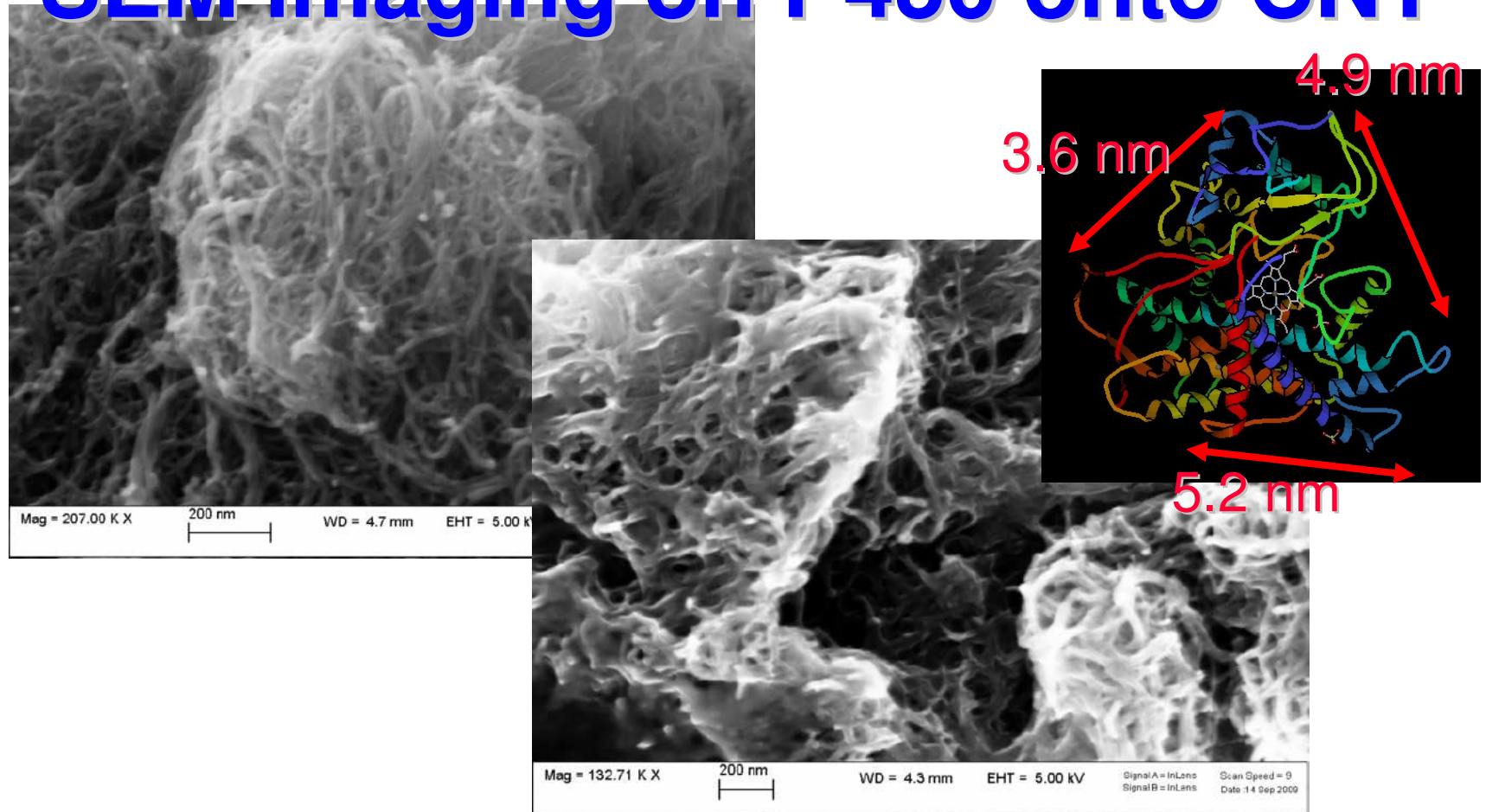
S. Joseph et al. / Biochemical Pharmacology 65 (2003) 1817–1826

Detection of verapamil by 3A4, an antihypertensive drug, was from 400 μM to 3mM while its therapeutic range is below 0.3 μM

An improved P450/Electrode coupling by using Carbon Nanotubes



SEM imaging on P450 onto CNT

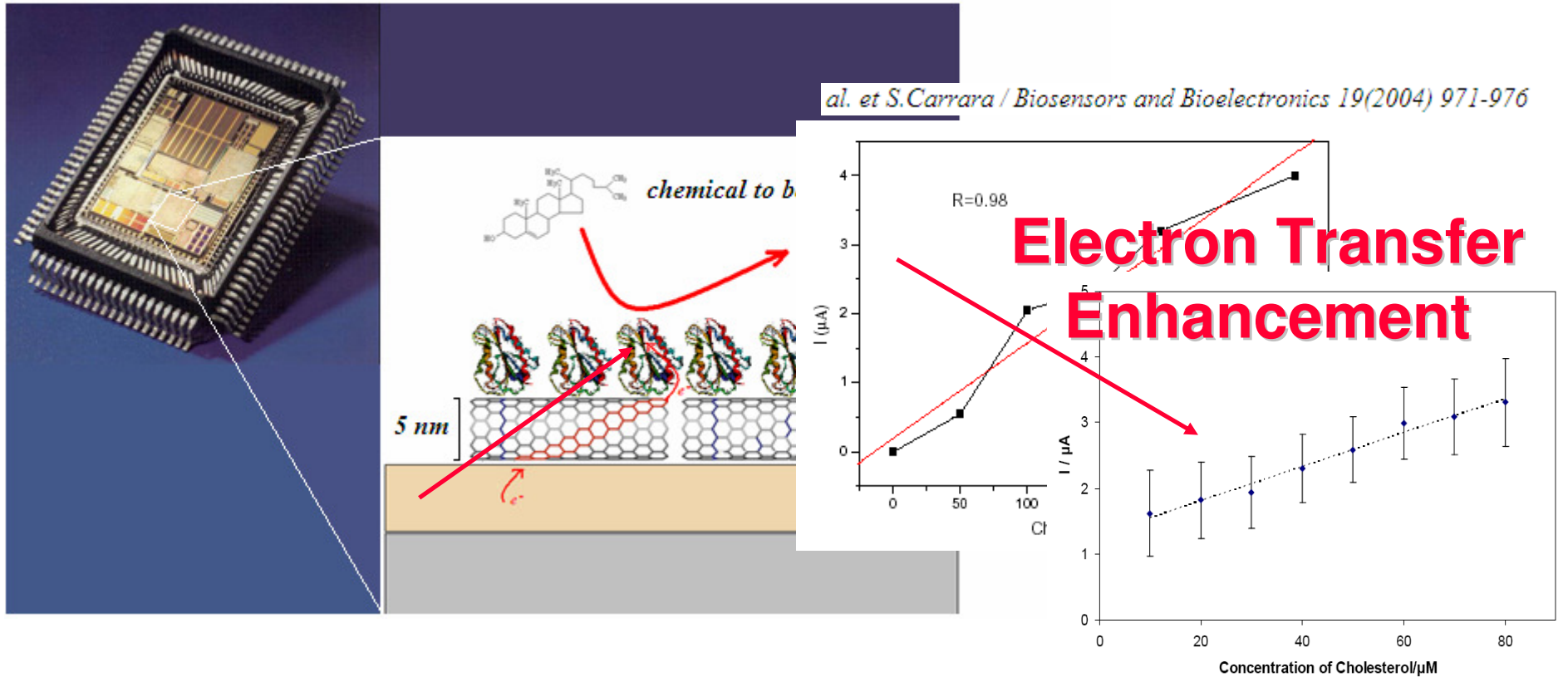


S. Carrara, et al., Biosensors and Bioelectronics (2010) submitted

Scanning Electron Microscopy clearly show the P450 wrapping onto each single Multi-Walled Carbon Nanotube

The improved Sensitivity

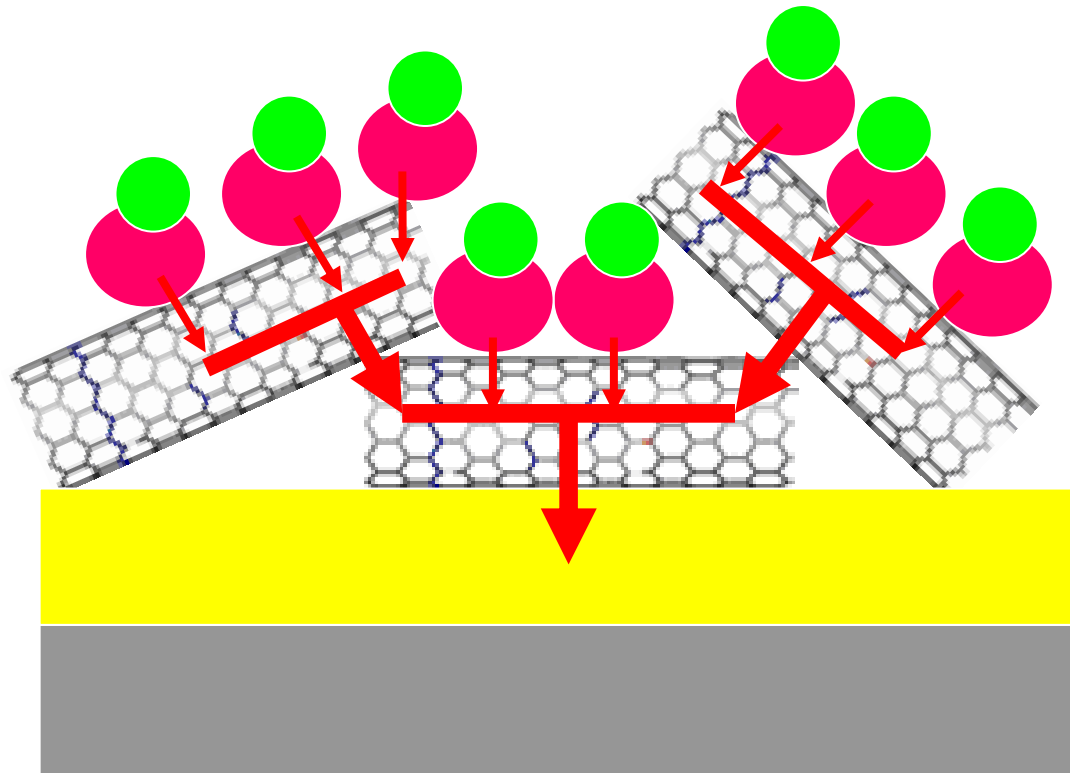
BIOSENSOR CHIP ARRAY



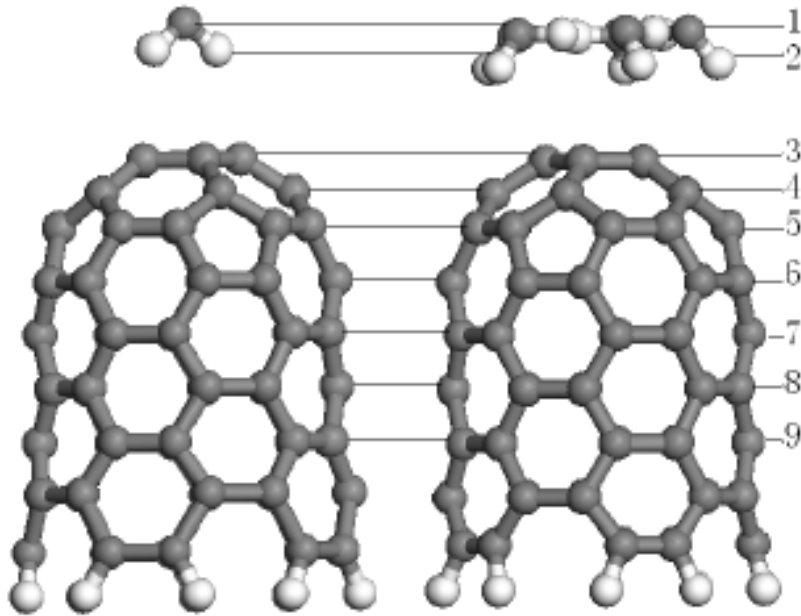
S.Carrara, et al., Biosensors and Bioelectronics 24 (2008) 148-150

The P450 11A1 performance in detecting Cholesterol is Enhanced by a factor 10x by using MWCNT

Drop casted CNT

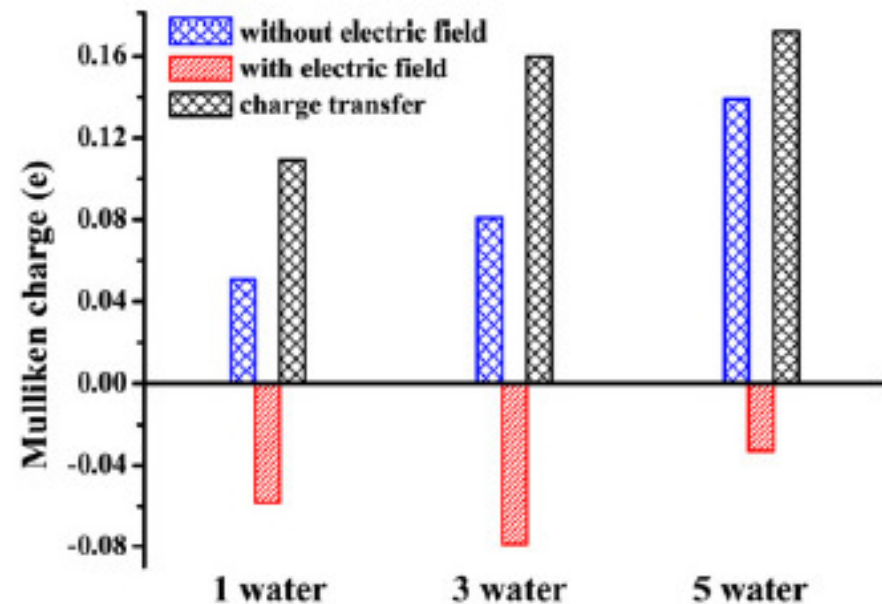


Emission from CNT in Water conditions



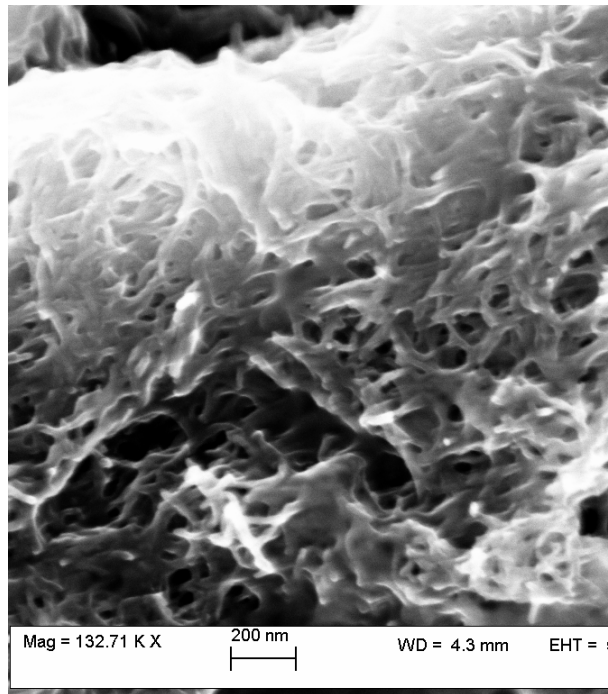
L Qiao *et al* Nanotechnology 18 (2007) 155707 (6pp)

**Water affects K-constants
in FN equation**

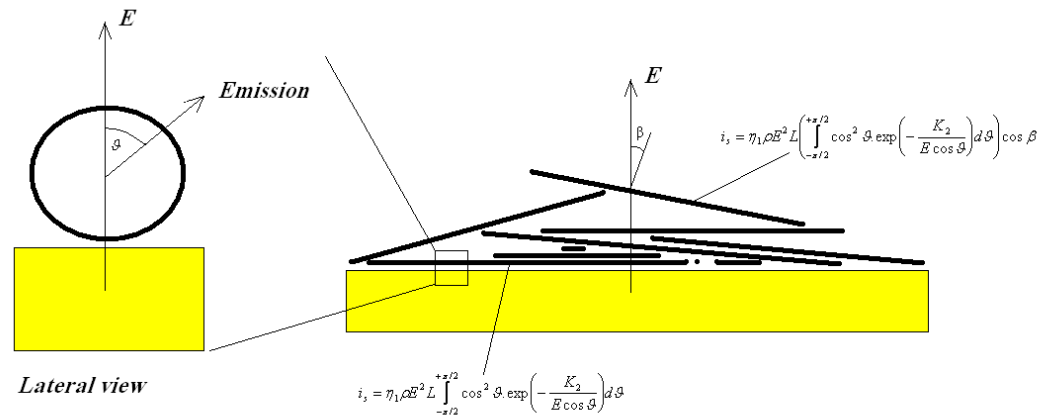
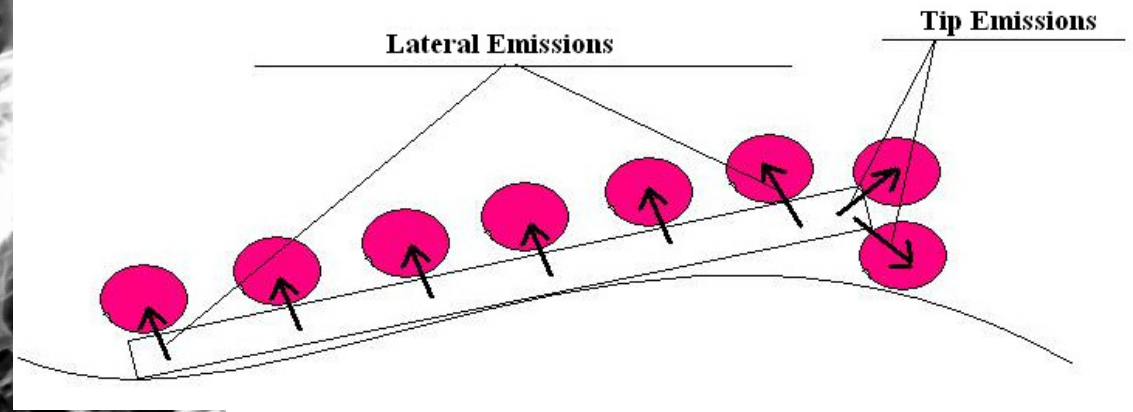


Electron emission from CNT is enhanced in presence of water molecules but a plateau is easily reached for few water molecules

CNT as quantum emitters

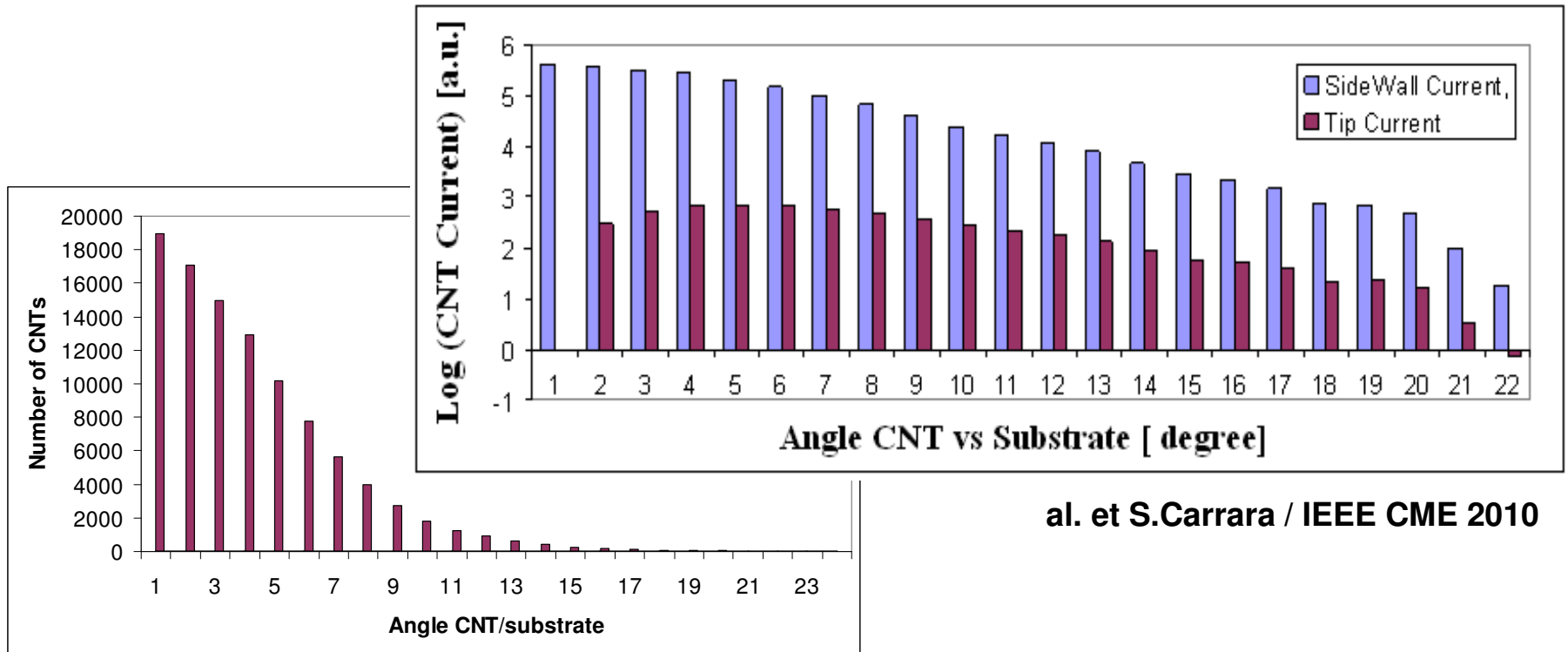


S.Carrara et al. / Unpublished



P450 proteins and MWCNTs deposited onto Screen-Printed electrodes and the models used for Monte-Carlo Simulations

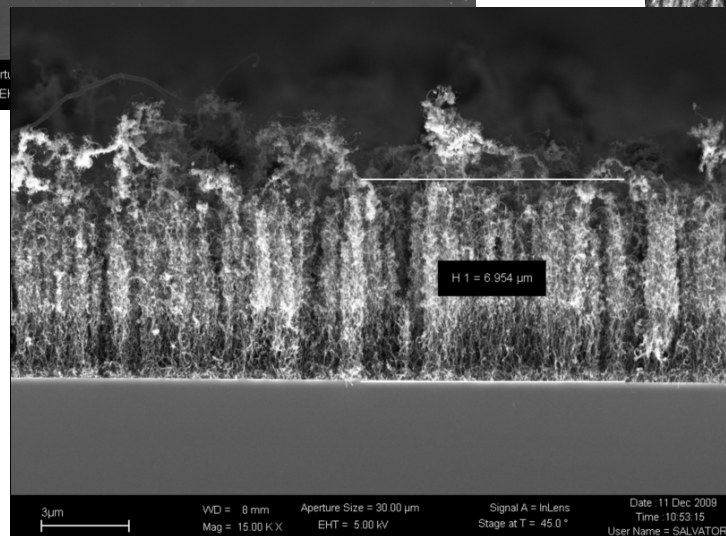
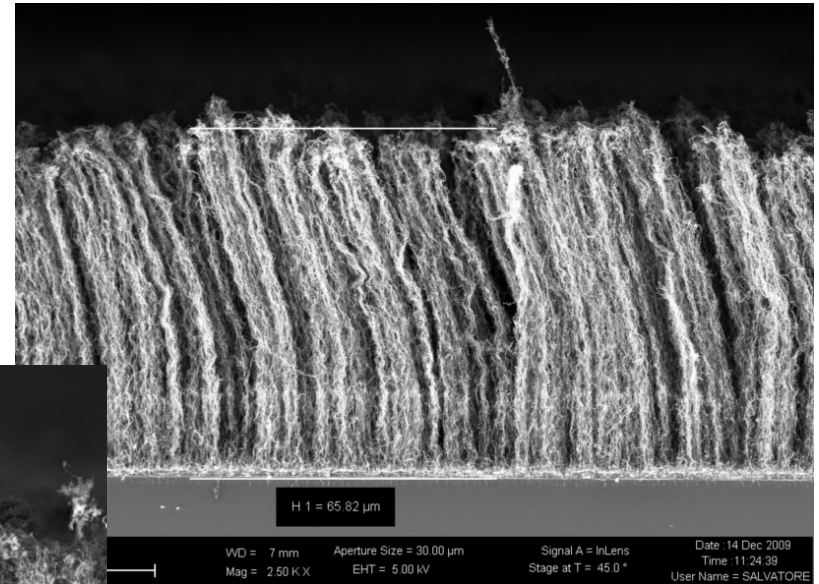
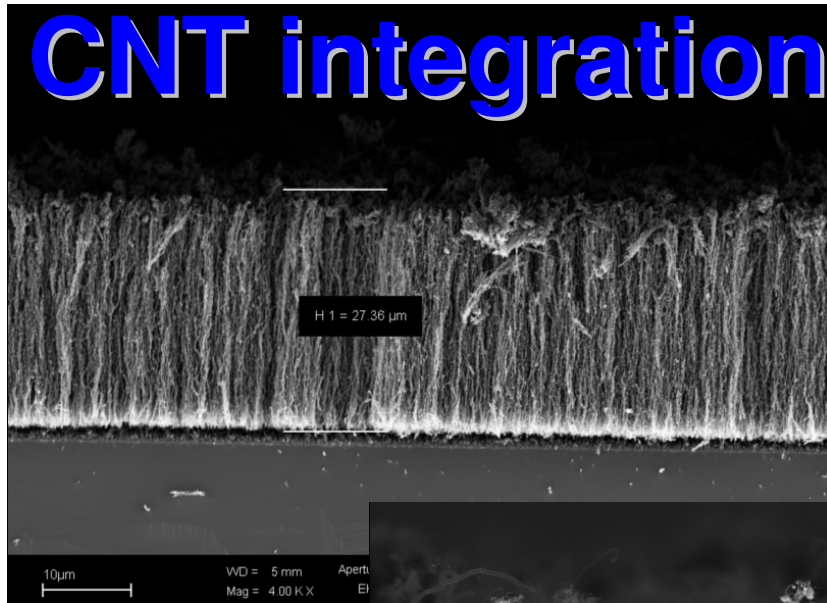
CNT randomly distributed and their Electron-Transfer



al. et S.Carrara / IEEE CME 2010

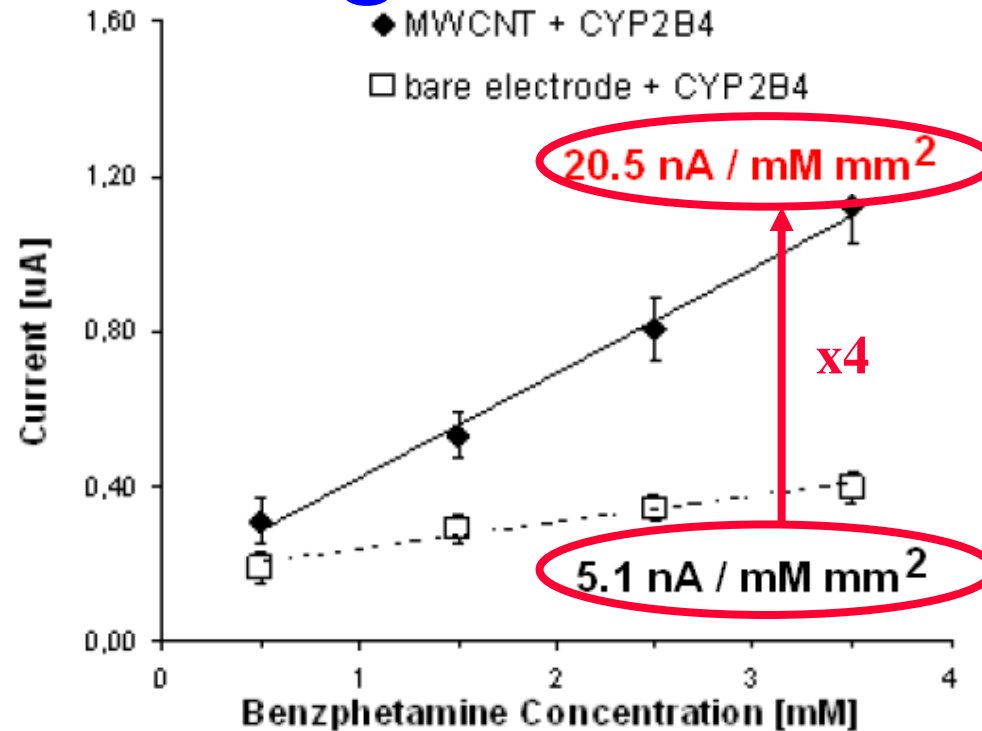
Distribution of CNTs randomly deposited on a corrugated substrate by Monte Carlo Simulations and comparison between lateral and tip Electrons-Transfer Emission

CNT integration directly onto Chip



Multi-Walled Carbon Nanotubes will be directly integrated onto the Silicon Substrate hosting the CMOS front-end required for the P450 based detection

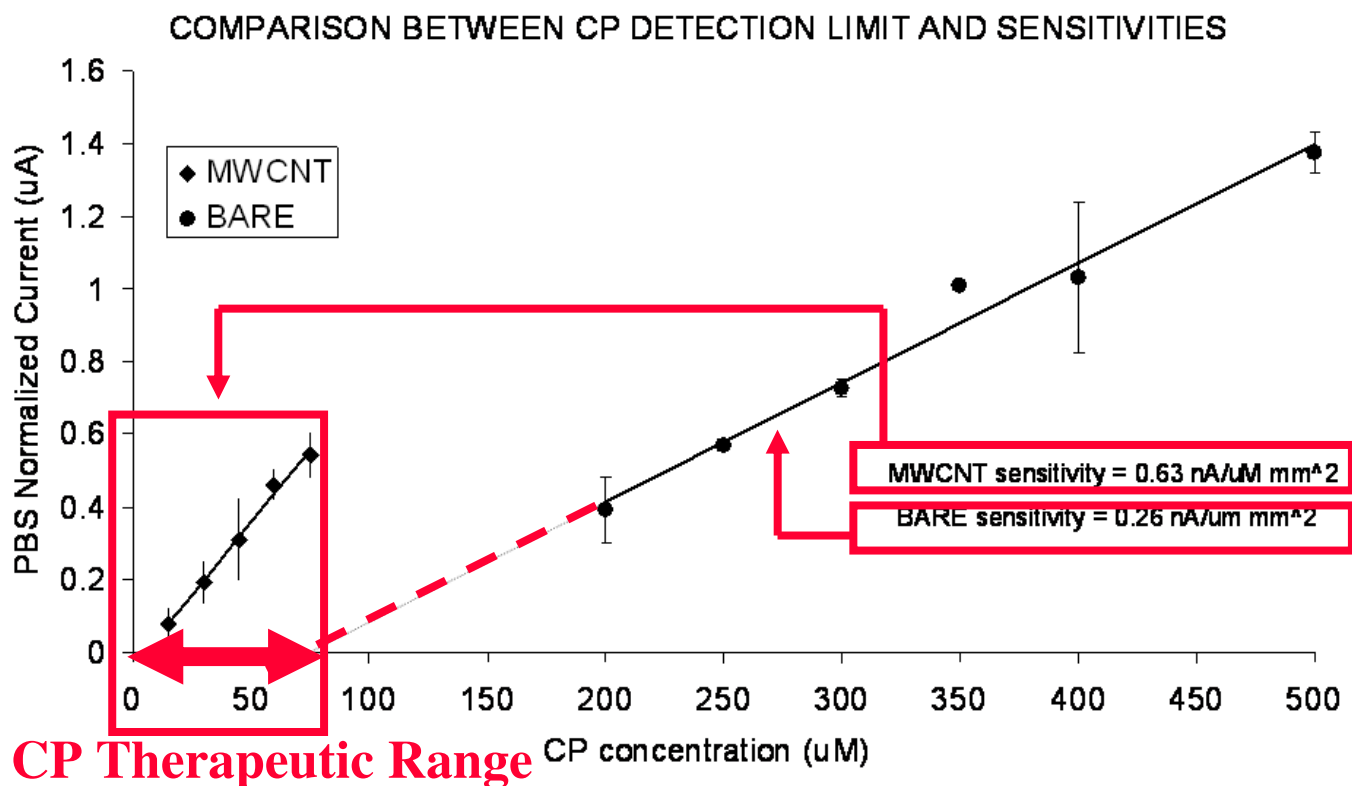
The improved sensitivity on Drugs detection



S. Carrara et al., Conference Proceedings of IEEE CME2009, Tempe (US), 9-11, April, 2009

P450 2B4 performance in detecting Benzphetamine is enhanced by a factor 4x by using MWCNT

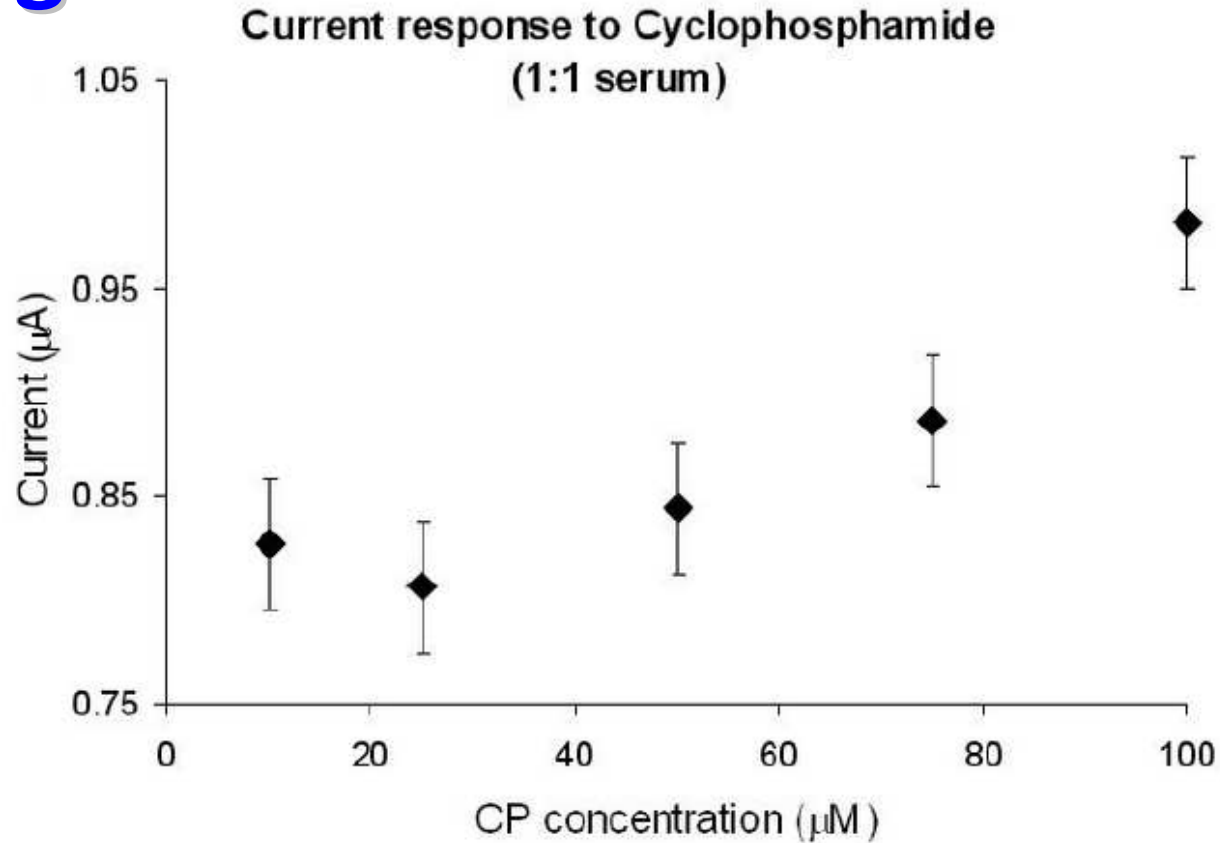
Improved Detection Limit on Drugs detection



S.Carrara et al. / unpublished

Cyclophosphamide (CP), an anti-cancer agent, is detected by P450 3A4 in its therapeutic range

Drugs detection in Human Serum



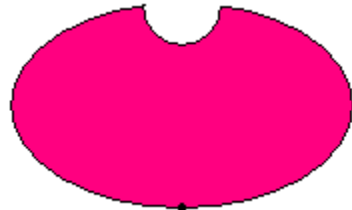
S.Carrara, et al., Biosensors and Bioelectronics (2010) submitted

Cyclophosphamide (CP) detected in Human Serum
within the therapeutic range

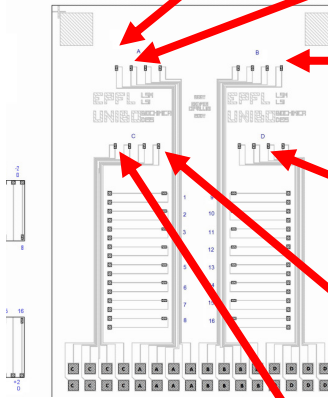
Drugs detection in the Pharmacological Range

Cytochrome	Drug	Measured Range (uM)	Therapeutic range (uM)	Best Sensitivity nA/uM mm ²
2B4	Benzphetamine	500-5000	0-0.074	2.14 (chronoamperometry)
	Amynopirine	100-500		0.01
3A4	Cyclophosphamide	0-500	2.6-76.6	0.63
	Dextromethorphan	100-500	0-0.3	0.12
	Erytromycin	0-75	0-68	0.26
2C9	Naproxen	100-500	21-515	0.25
	Ibuprofen	100-500	0.48-291	0.03
	Flurbiprofen	100-500	0.04-41	0.08

Applications in Cardiovascular therapy



CYP cytochromes	Drugs principles	Endogenous metabolic molecules
2C9	Hypoglycemic agents Angiotensin Blockers,	
2D6	Beta blockers	
2B4	Anti-obesity	
3A4,5,7	HMG CoA Reductase Inhibitors, Anti-arrhythmics, Calcium channels blockers	testosterone
11A1		Cholesterol
4A11		Arachidonic acid
5A1		thromboxane A ₂ synthase



Applications in Breast Cancer

Drugs	Pharmacological concentration	CYP involved in drug metabolism ⁽¹⁾
Cyclophosphamide ^{(2),(3)}	2,68-76,6 μM	2C9 (-)
Etoposide ^{(4),(5)}	33,98-101,94 μM	3A4 1A2 (-)
Ifosfamide ⁽²⁾	10-160 μM	3A4 2B6
Mitoxantrone ⁽⁶⁾	1,84-3,31 μM	3A4 1B1 (-)
Tegafur ⁽⁷⁾ (contain Fluorouracil)	1 μM -10 μM	1A2 2A6

Good concentration ranges for the sensitivity of our technology !

The CYP in the table are sorted according to their importance in the drug metabolism.

The symbol (-) means that the CYP isoform is involved as the minor enzymatic components in the drug metabolic pathway.

Breast cancer drugs cocktail

- cyclophosphamide, methotrexate, and fluorouracil (CMF)⁽⁸⁾⁽¹¹⁾;
- fluorouracil, doxorubicin, and cyclophosphamide (FAC)⁽⁸⁾;
- cyclophosphamide, doxorubicin and 5-fluorouracil (CAF)⁽⁹⁾;
- fluorouracil, epirubicin, and cyclophosphamide (FEC)⁽⁸⁾⁽¹¹⁾⁽¹²⁾;
- fluorouracil, doxorubicin, and cyclophosphamide ⁽¹¹⁾⁽¹²⁾;
- Ifosfamide, Carboplatin, Etoposide (ICE)⁽⁹⁾;
- ifosfamide , metho- trexate and 5-fluorouracil (IMF)⁽⁹⁾;
- cyclophosphamide, mitoxantrone, and etoposide⁽¹²⁾.

[8] New England Journal of Medicine, The [0028-4793] Hortobagyi yr:1998 vol:339 iss:14 pg:974
GABRIELN. HORTOBAGYI, M.D.

[9] Cancer Chemother Pharmacol (1999) 44 (Suppl): S26±S28

A.Y. Chang, L. Hui, R. Asbury, L. Boros, G. Garrow, J. Rubins

[10] *Journal of Clinical Oncology*, Vol 22, No 12 (June 15), 2004: pp. 2284-2293

M. Ayers, W.F. Symmans, J. Stec, A.I. Damokosh, E. Clark, K. Hess, et al.

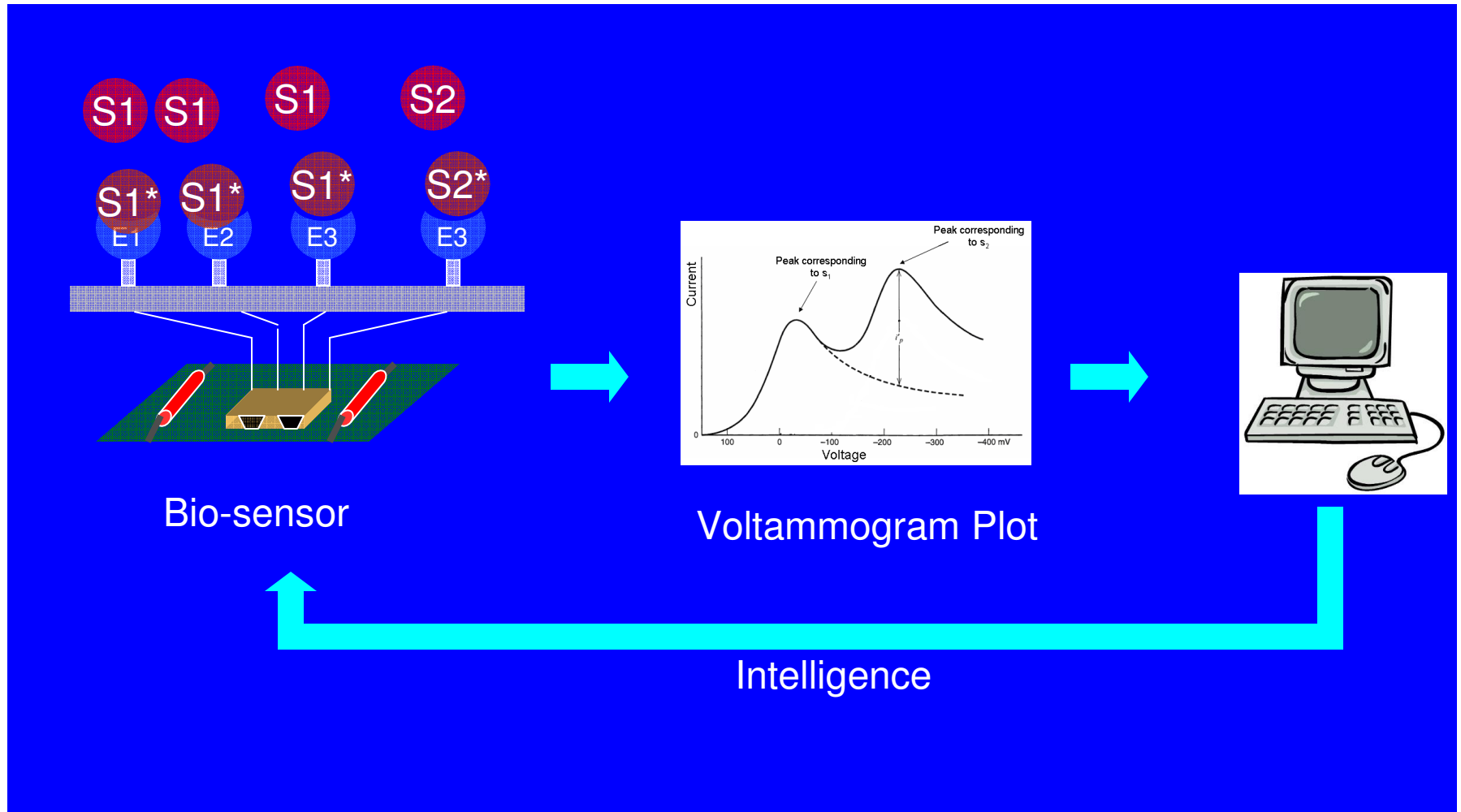
[11] *Journal of Clinical Oncology*, Vol 21, Issue 13 (July), 2003: 2600-2608

Manfred Kaufmann, Gunter von Minckwitz, Roy Smith, Vicente Valero, et al

[12] *The Lancet* [0140-6736] Weiss yr:2000 vol:355 iss:9208 pg:999

Raymond B Weiss, Robert M Rifkin, F Marc Stewart, Richard L Theriault, et al.

The Problem of multi-panel arrays response



Different Drugs give peaks in different positions

Substrate/inhibitor of CYP2C9	K_m (μM)	K_i (μM)	CYP2C9 (mV)	E_{mid} CYP2C9 + substrate (mV)
Torsemide (s)	11.4		-41	-19
Diclofenac (s)	6.8		-41	-41
Tolbutamide (s)	120 ^a		-41	-37
S-Warfarin (s)	6 ^b		-41	-36
Sulfaphenazole (i)		0.1 ^c	-41	-41
CO _(g)			-41	8

D.L. Johnson et al. / Biochemical Pharmacology 69 (2005) 1533–1541

$$i(V) = i_c(V) + \sum_{\forall k} A_k e^{-\frac{(V-V_k)^2}{\sigma_k^2}}$$

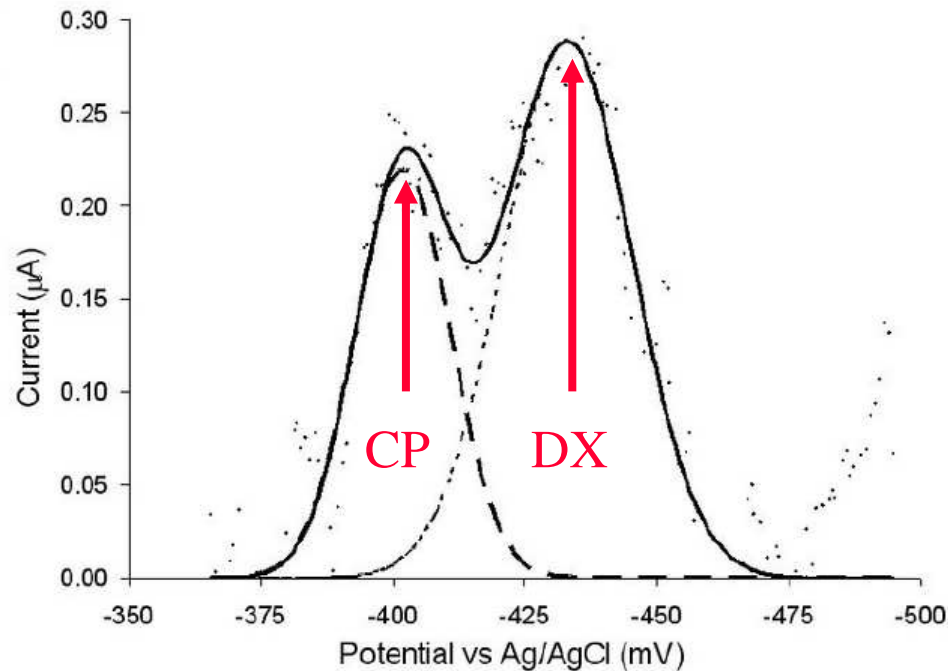
↑ Charging current ↑ Faradic currents

The cytochrome P450 2C9 presents peak shifts in the range of tens of mV by changing drug substrates

Multiple-Drugs Detection

S. Carrara et al., Conference Proceedings of IEEE CME2009, Tempe (US), 9-11, April, 2009

P450-2B4	P450-3A4
Benzphetamine (BZ) - anti-obesity	Cyclophosphamide (CP) - anti-cancer agent
7-nitoxypresorufin (PX) - anti-obesity	Dextromethorphan (DX) - analgesic
	Midazolam (MZ) - Anticonvulsant/sedative

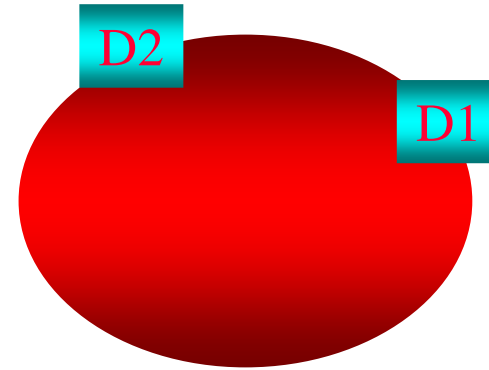


S. Carrara, et al., Biosensors and Bioelectronics (2010) submitted

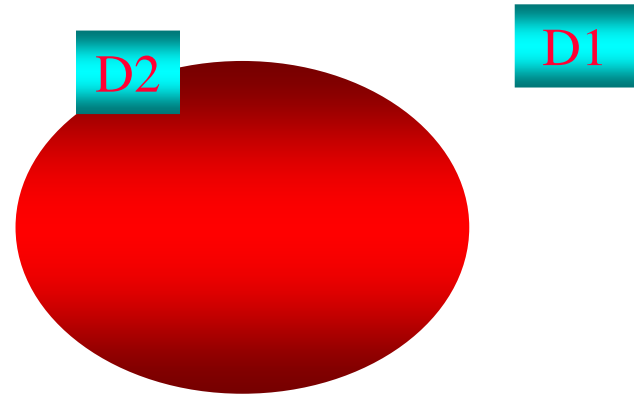
The same P450 may detects more drug compounds

The Heterotropic Kinetics

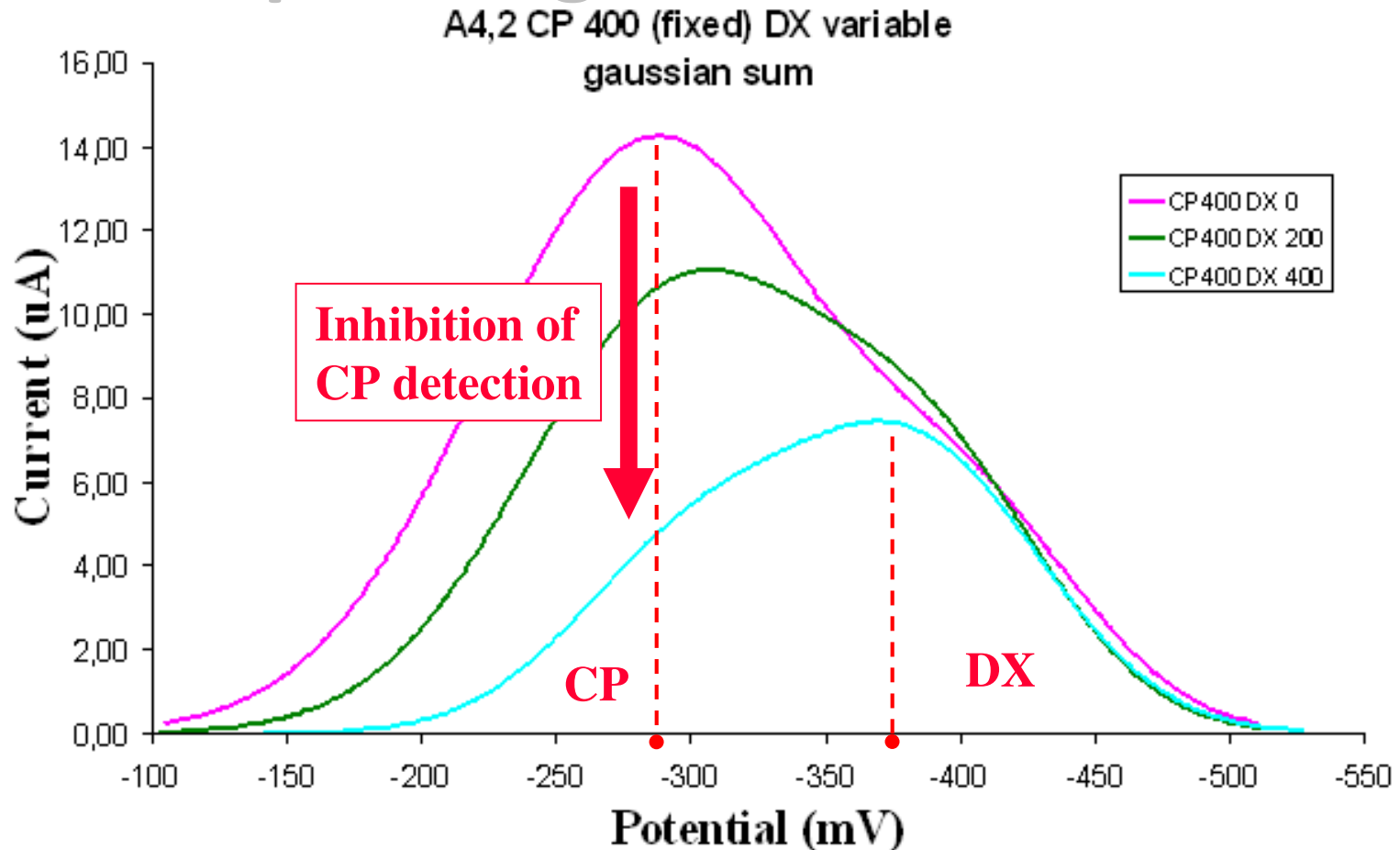
- **HETERO ACTIVATION**



- **PARTIAL INHIBITION**

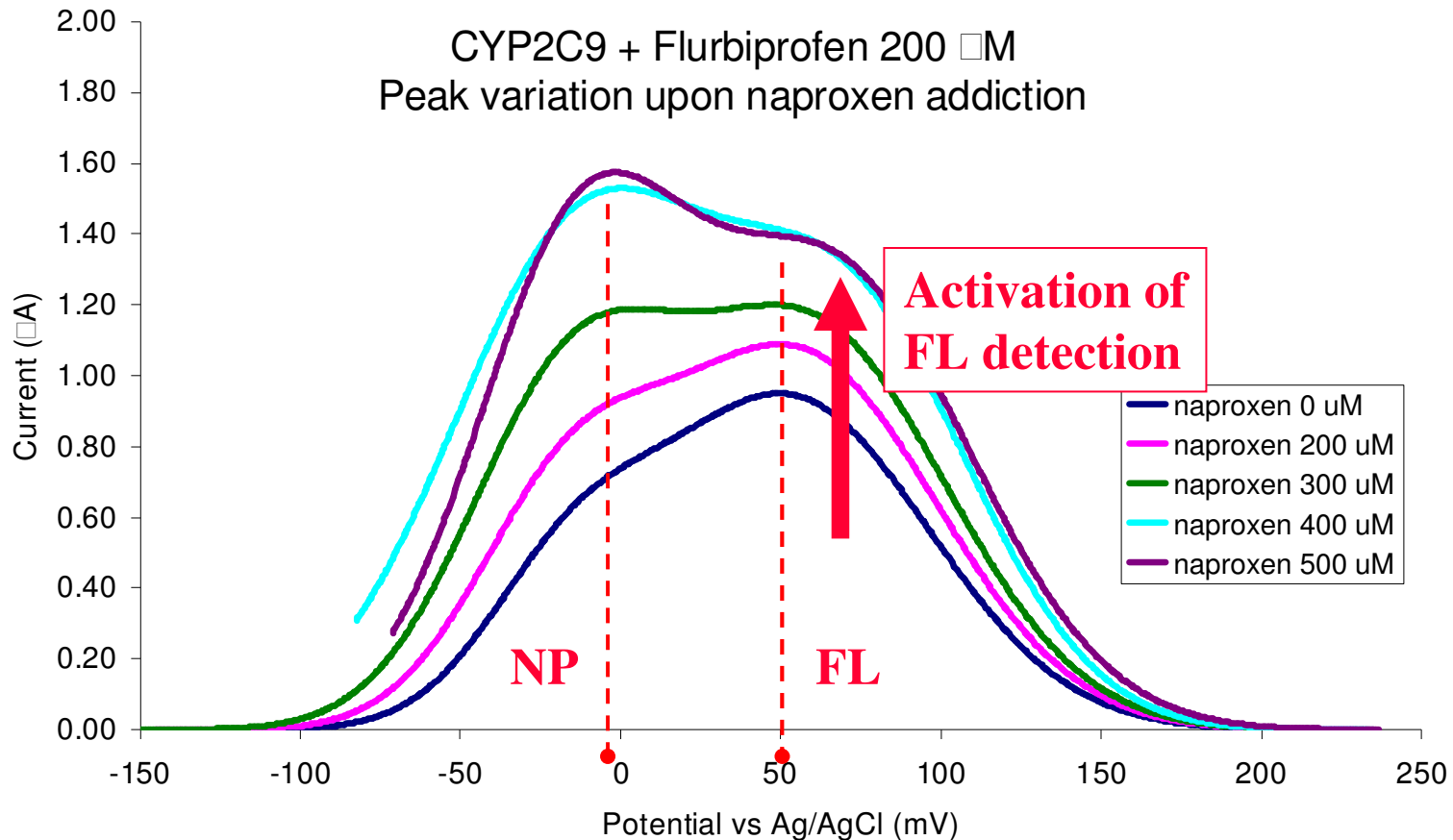


Multiple drugs detection: CYP3A4



Different amounts of CP and DX result in two very-well defined peaks once detected by P450 3A4

Multiple drugs detection: CYP2C9



Naproxen (NP) and Flurbiprofen (FL) also result in two very-well defined peaks once detected by P450 2C9

Peaks Amplitude is affected by the other drugs

Substrate/inhibitor of CYP2C9	K_m (μM)	K_i (μM)	CYP2C9 (mV)	E_{mid} CYP2C9 + substrate (mV)
Torsemide (s)	11.4		-41	-19
Diclofenac (s)	6.8		-41	-41
Tolbutamide (s)	120 ^a		-41	-37
S-Warfarin (s)	6 ^b		-41	-36
Sulfaphenazole (i)		0.1 ^c	-41	-41
CO _(g)			-41	8

Dependence from the other drug concentrations

D.L. Johnson et al. / Biochemical Pharmacology 69 (2005) 1533–1541

$$i(V) = i_C(V) + \sum_{\forall k} \prod_{\forall j \neq k} A_k([c_j]) e^{-\frac{(V-V_k)^2}{\sigma_k^2}}$$

Charging current

Faradic currents

The Gaussian decomposition in cytochrome P450 based detection has to account for the heterotropic kinetics

A general approach

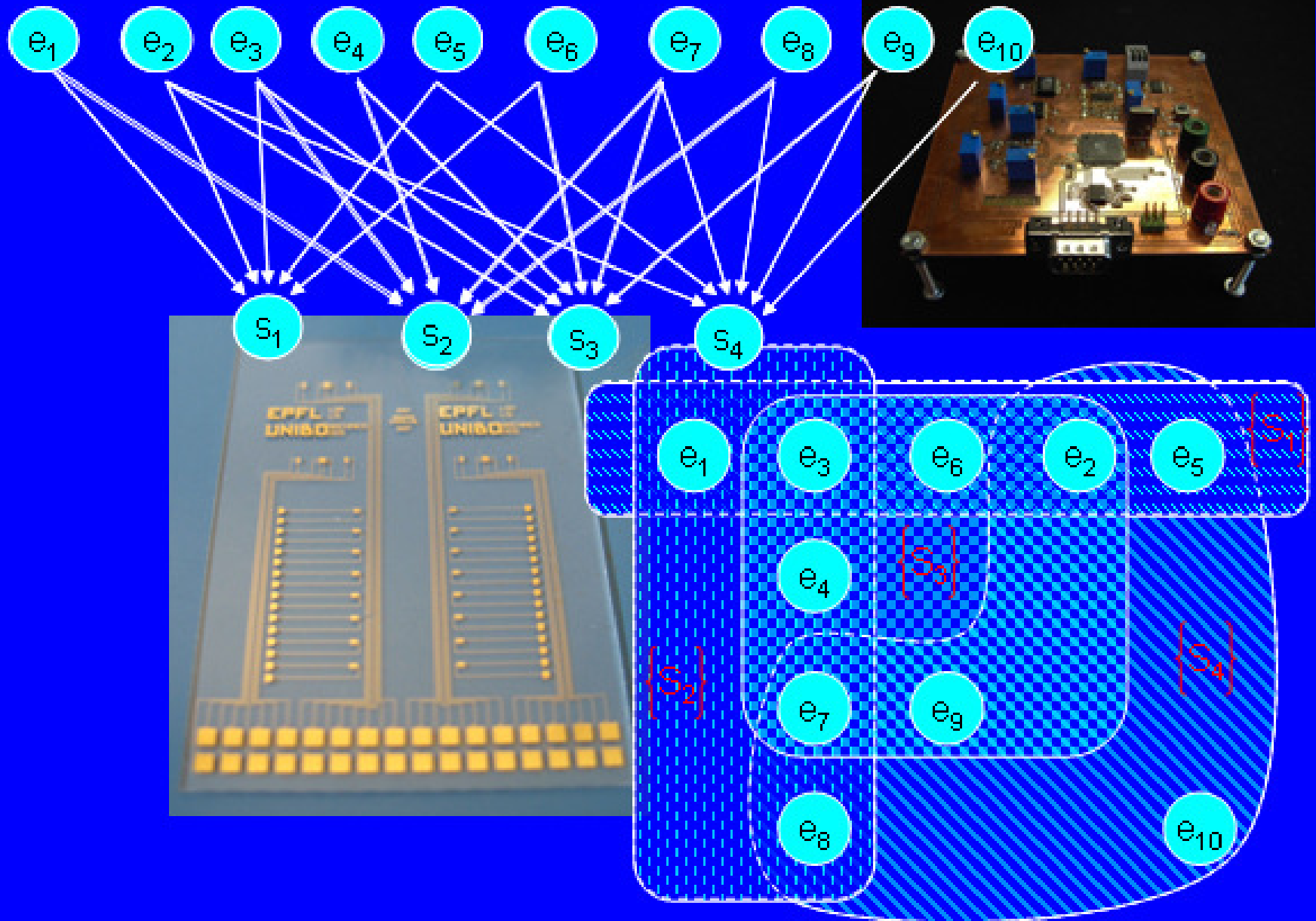
$$i(V) = i_c(V) + \sum_{\forall k} \prod_{\forall j \neq k} A_k([C_j]) e^{-\frac{(V-V_k)^2}{\sigma_k^2}}$$

$$A_k([C_j]) = A_{k0} nFAD \left(\frac{nFvD_k}{RT} \right)^{1/2} C_k \left(\frac{1}{1 + e^{2\varepsilon_j(C_j - C_{0j})}} \right)$$

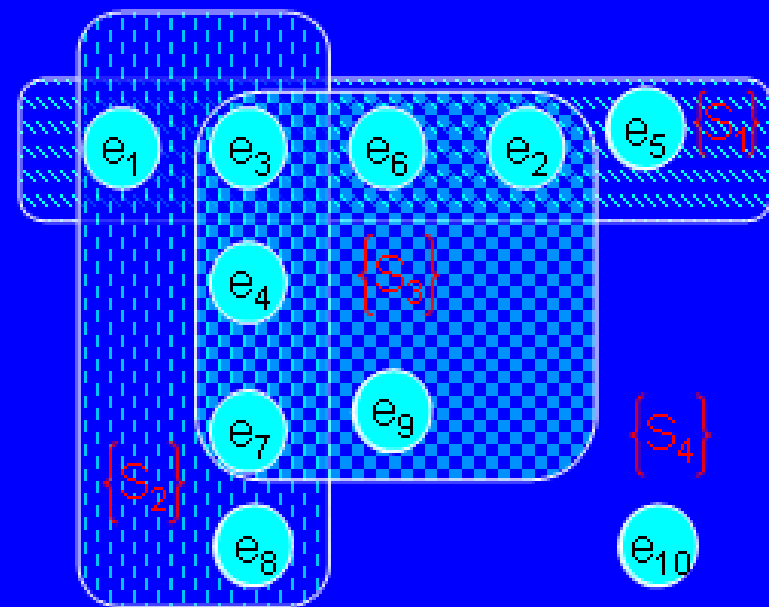
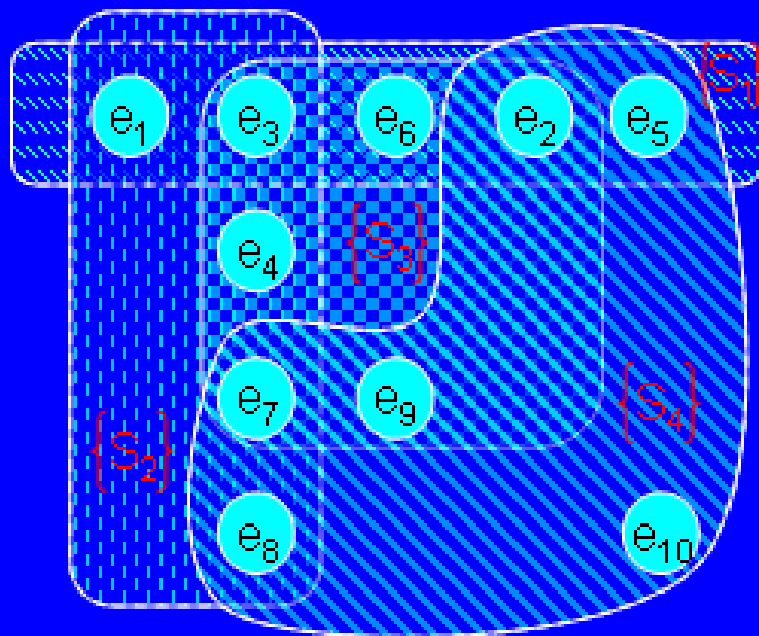
$$A_k([C_j]) = A_{k0} nFAD \left(\frac{nFvD_k}{RT} \right)^{1/2} C_k \left(1 - \frac{1}{1 + e^{2\varepsilon_j(C_j - C_{0j})}} \right)$$

A general approach for multi-peak decomposition is required for hetero activation and partial inhibition

Further Perspective: multi-panel biochip



The irredundant Cover problem



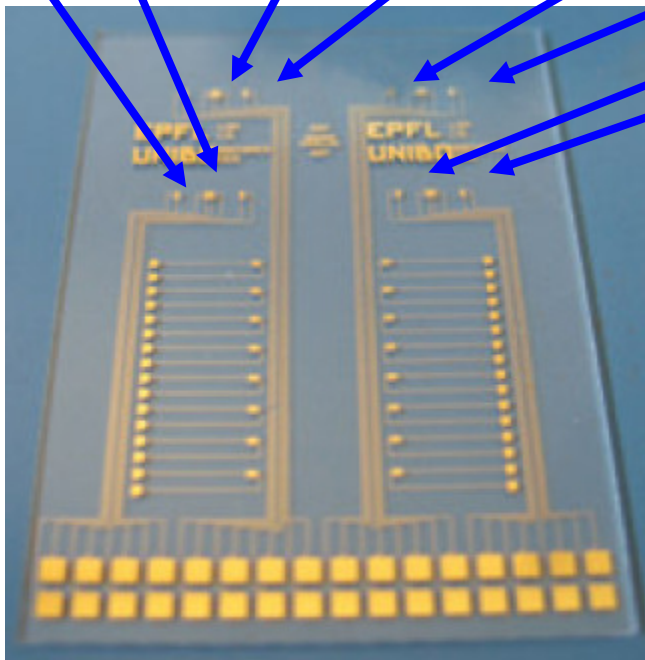
Irredundant Cover set $\{s_1, s_2, s_3\}$

Solution of the irredundant cover problem provides improved specificity at system level

Sensor array architecture

Probe enzymes

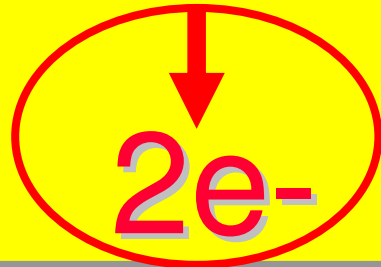
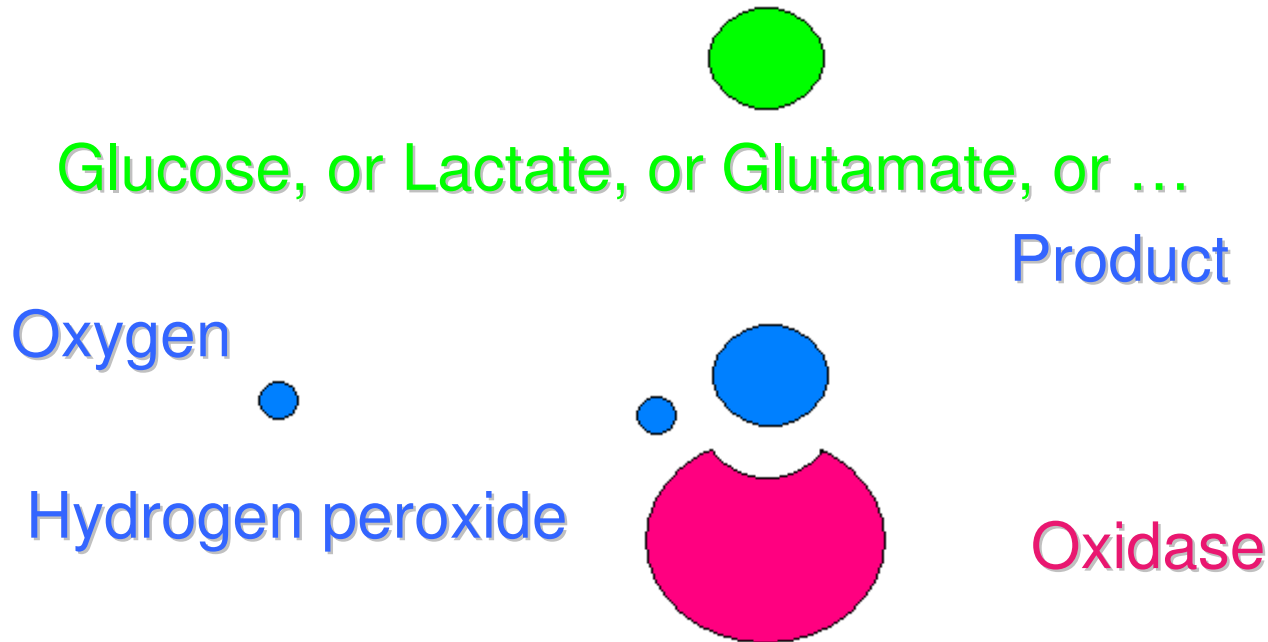
ATP-ase	Lactate oxidase	Glucose oxidase	Lipoxygenase
P450 11A1	P450 5A1	P450 4A11	Cholesterol oxidase



- Glucose
- Lactate
- Cholesterol
- Triglycerides
- Drugs

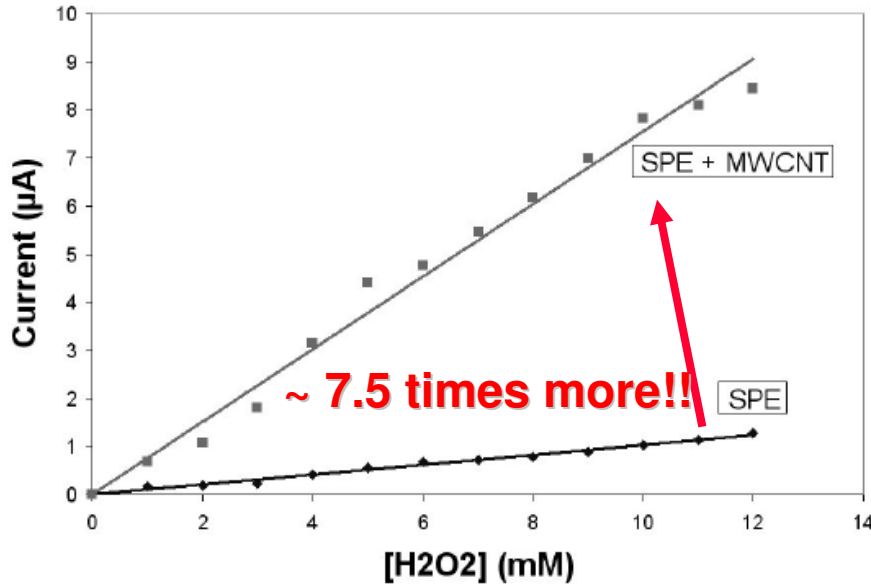
Different enzymes sense different target metabolites

Working principle of Oxidases based detection



Amperometric
Detection !!!!!

Peroxide Detection



C.Boero, S.Carrara, et al., best paper @ IEEE Prime 2009

TABLE I
SENSITIVITY VALUES FROM LITERATURE

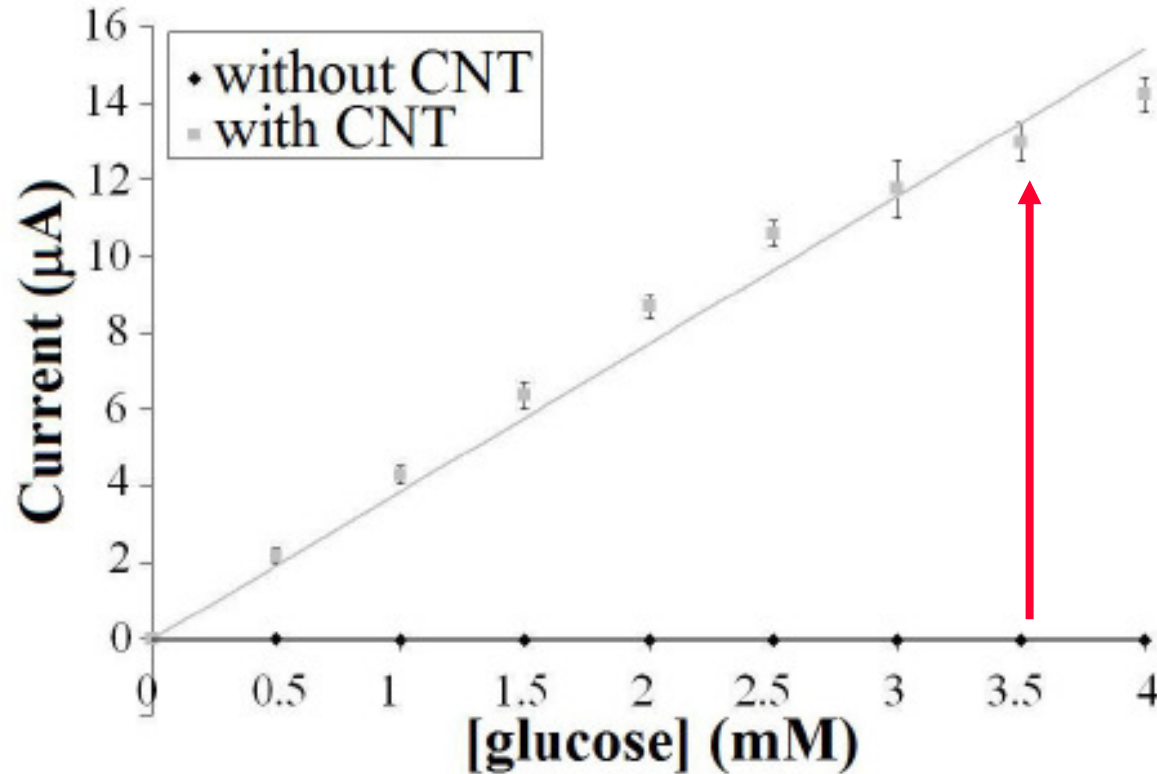
Methods	Sensitivity
Au-Nafion®- TNTs [11]	0.24 $\mu\text{A mM}^{-1} \text{cm}^{-2}$
Polypyrrole - polyanion/PEG [12]	0.5 $\mu\text{A mM}^{-1} \text{cm}^{-2}$
MWCNT-chitosan [13]	8.3 $\mu\text{A mM}^{-1} \text{cm}^{-2}$
chitosan/PVI-Os/CNT [9]	19.7 $\mu\text{A mM}^{-1} \text{cm}^{-2}$

2 order of magnitude!!!

- [9] X. Cui, *Biosensors and Bioelectronics*, vol. 22, pages 3288-3292, 2007
- [11] M. Yang, *Nanotechnology*, vol. 19, page 075502, 2008
- [12] W.J. Sung, *Sensors and Actuators B*, vol. 114, pages 164-169, 2006
- [13] Y. Tsai, *Sensors and Actuators B*, vol. 125, pages 474-481, 2007

The peroxide detection is highly improved
by using carbon nanotubes

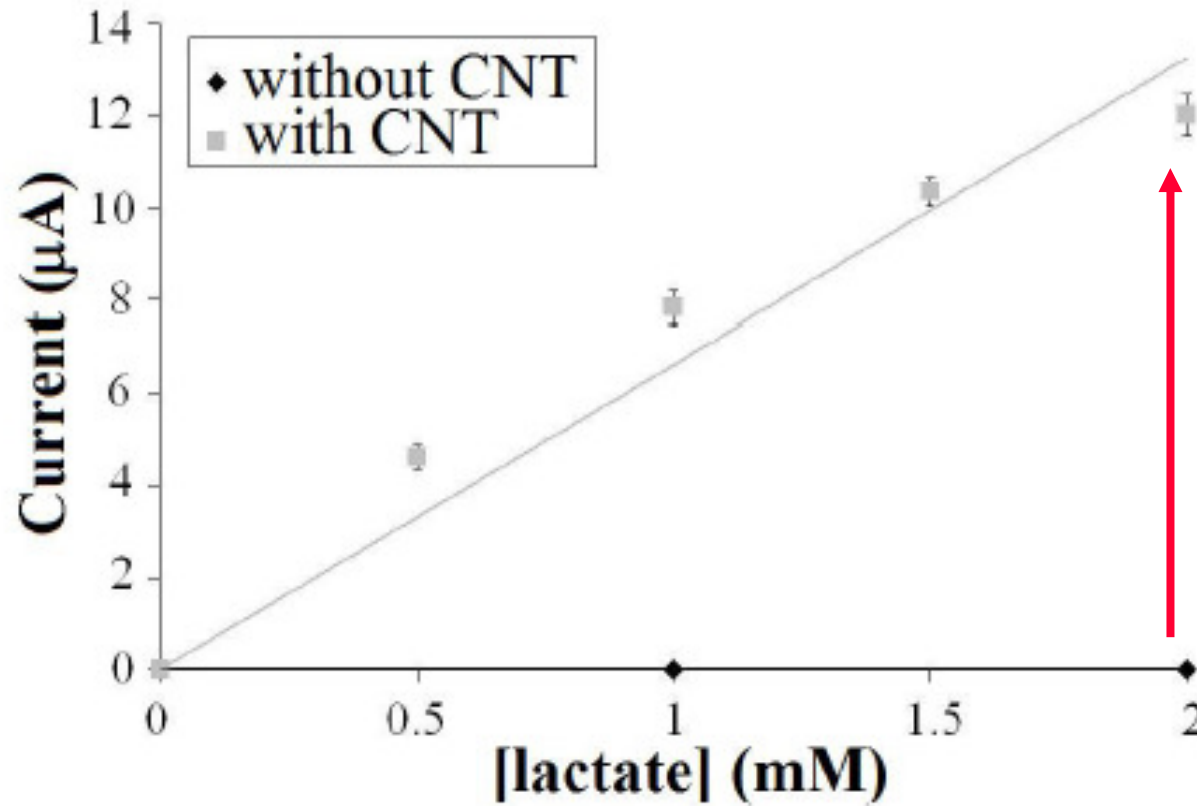
Glucose Detection



C.Boero, S.Carrara et al. / IEEE CME 2010, submitted

The Glucose detection is highly improved
by using carbon nanotubes

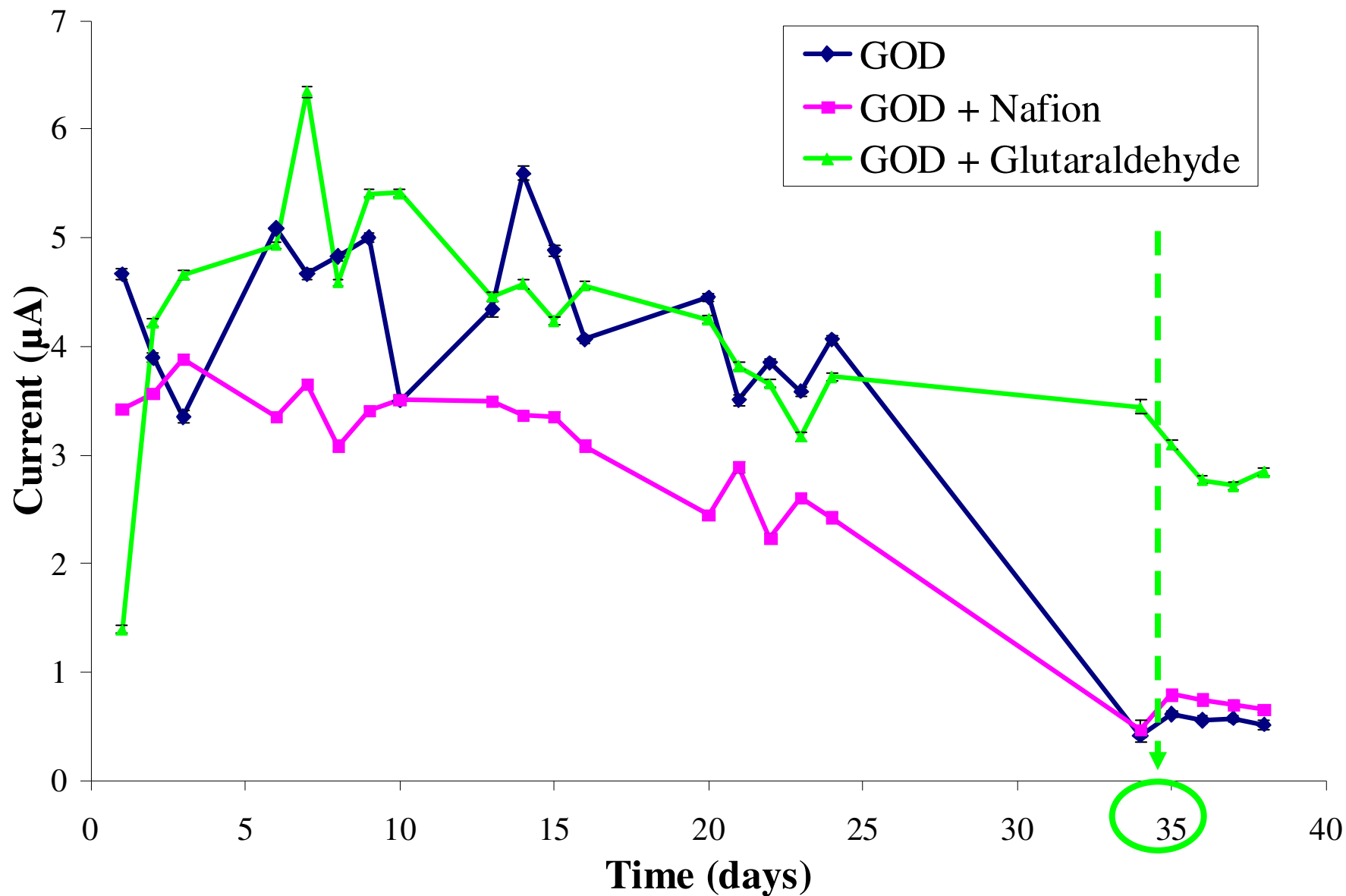
Lactate Detection



C.Boero, S.Carrara et al. / IEEE CME 2010, submitted

The Lactate detection is highly improved
by using carbon nanotubes

Detection of 4 mM of glucose



Time stability of sensors in RAT experiments

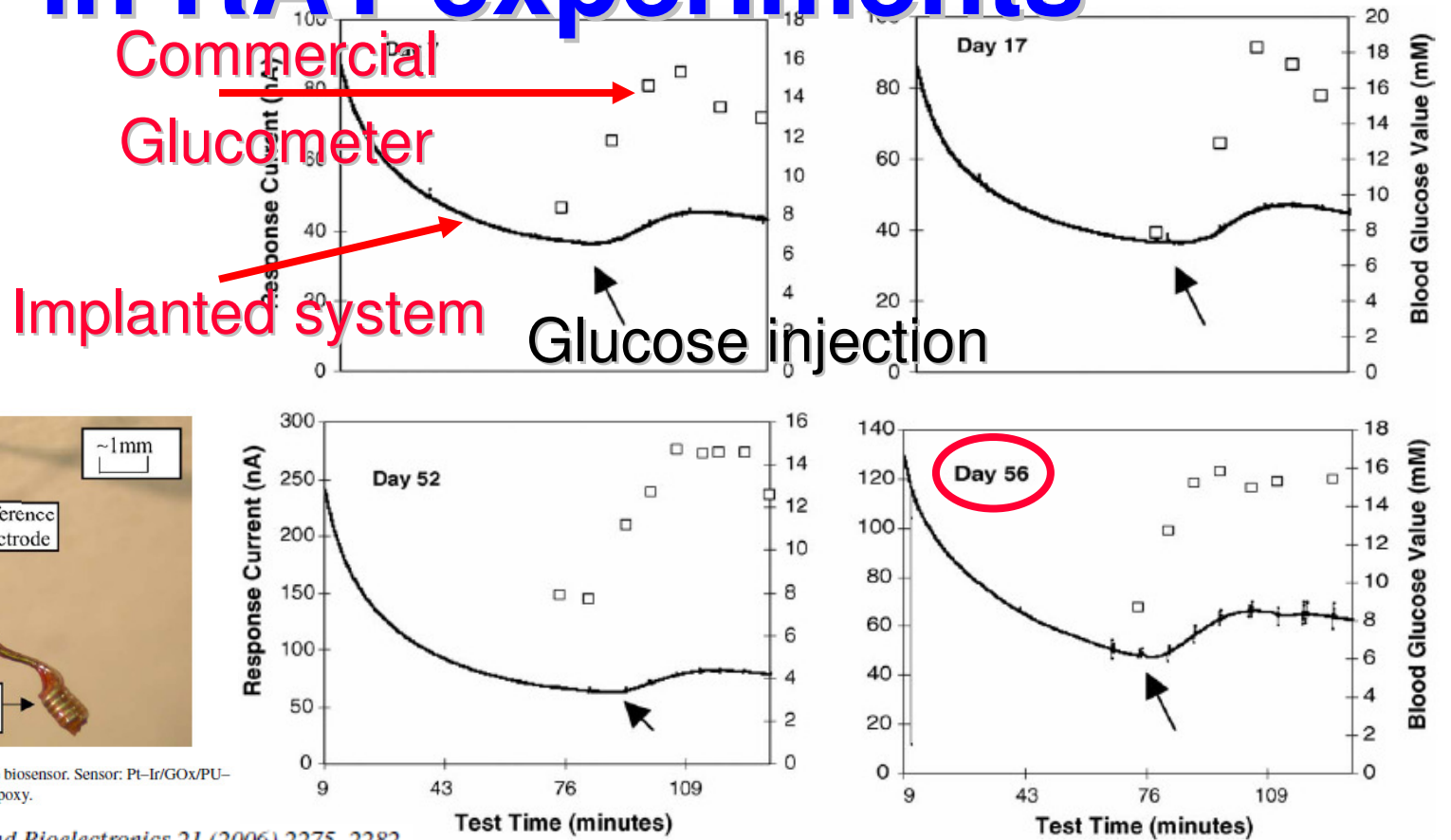
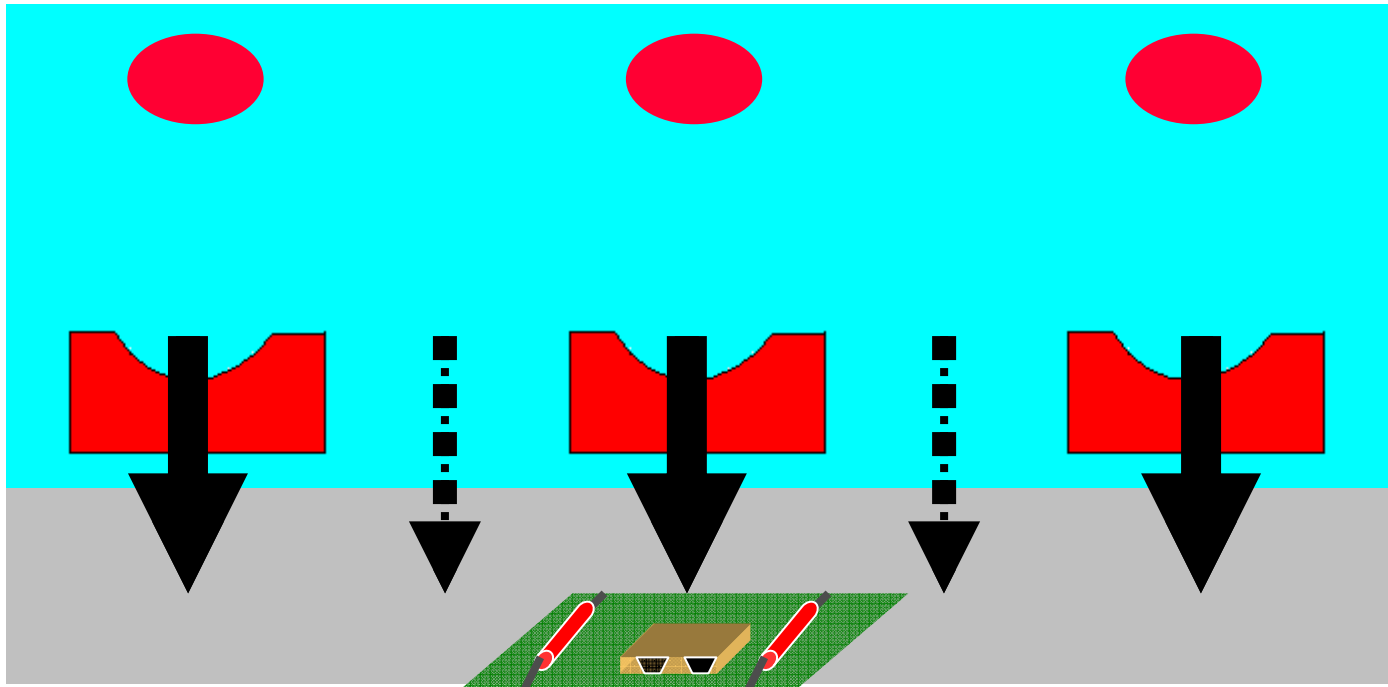


Fig. 1. A picture of the implantable glucose biosensor. Sensor: Pt-Ir/GOx/PU-epoxy; reference electrode: Ag/AgCl/PU-epoxy.

B. Yu et al. / Biosensors and Bioelectronics 21 (2006) 2275–2282

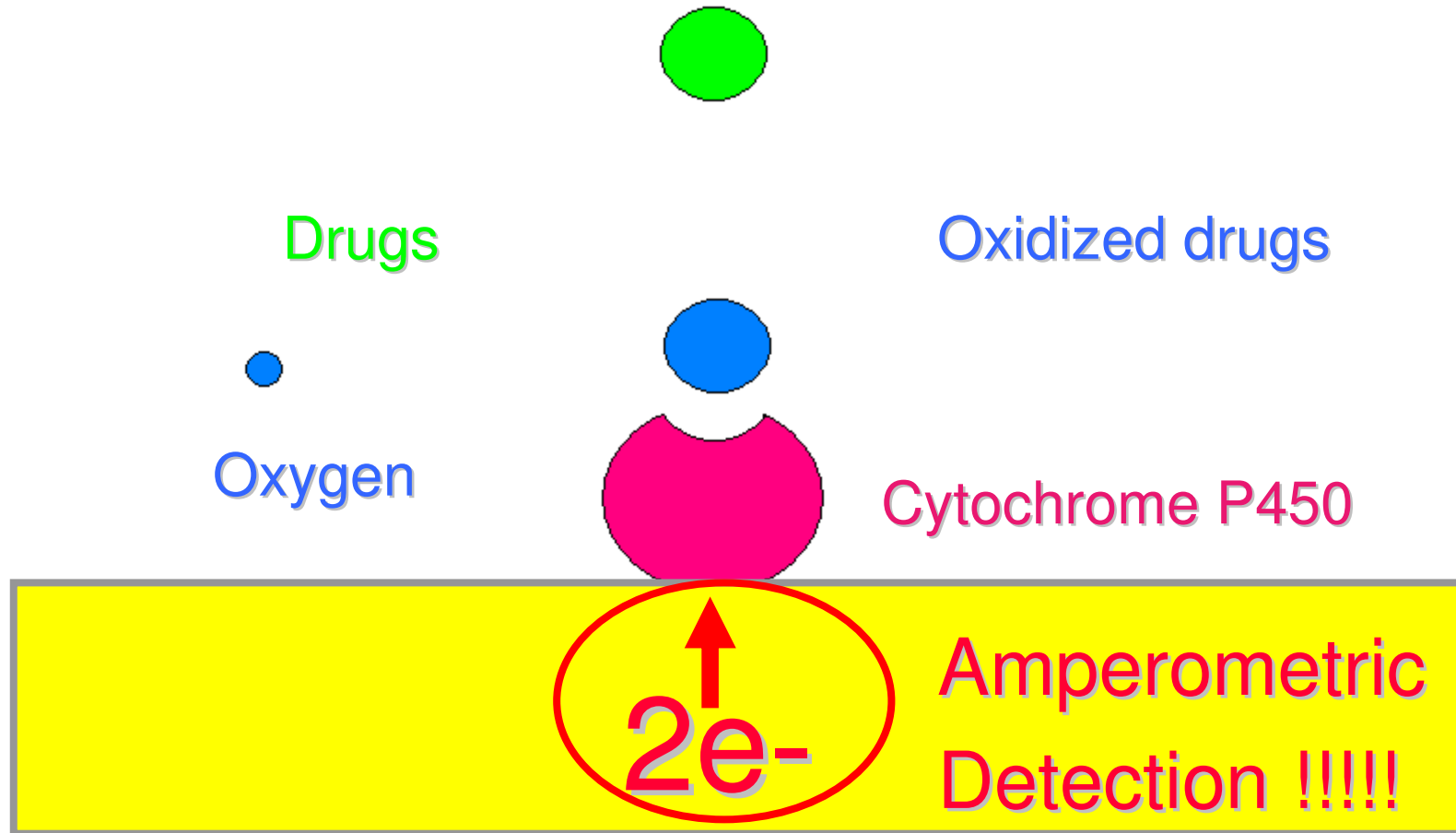
The epoxy-enhanced polyurethane membranes provide long-term stability for implanted biochip

Bio/CMOS interface

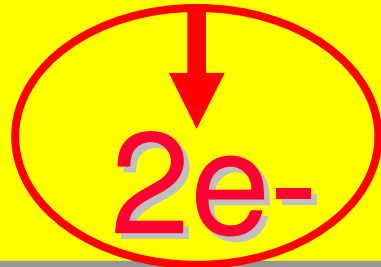
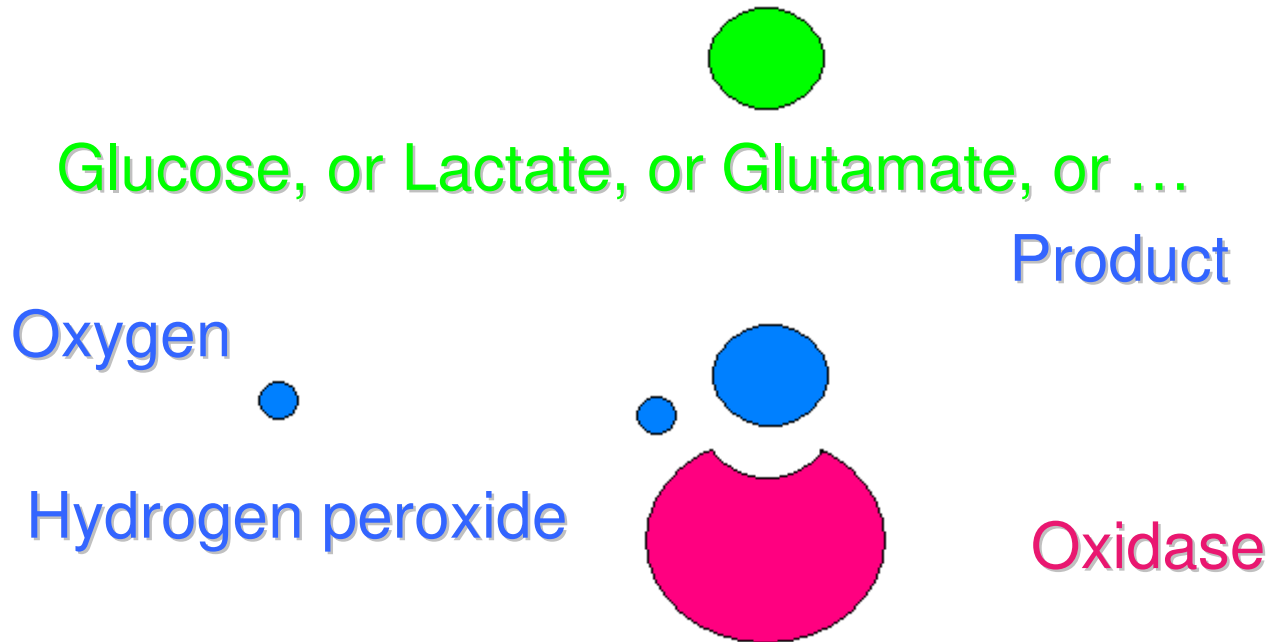


The interface between the CMOS circuit and the bio sample needs to be deeply investigated before design

Working principle of P450-based Detection

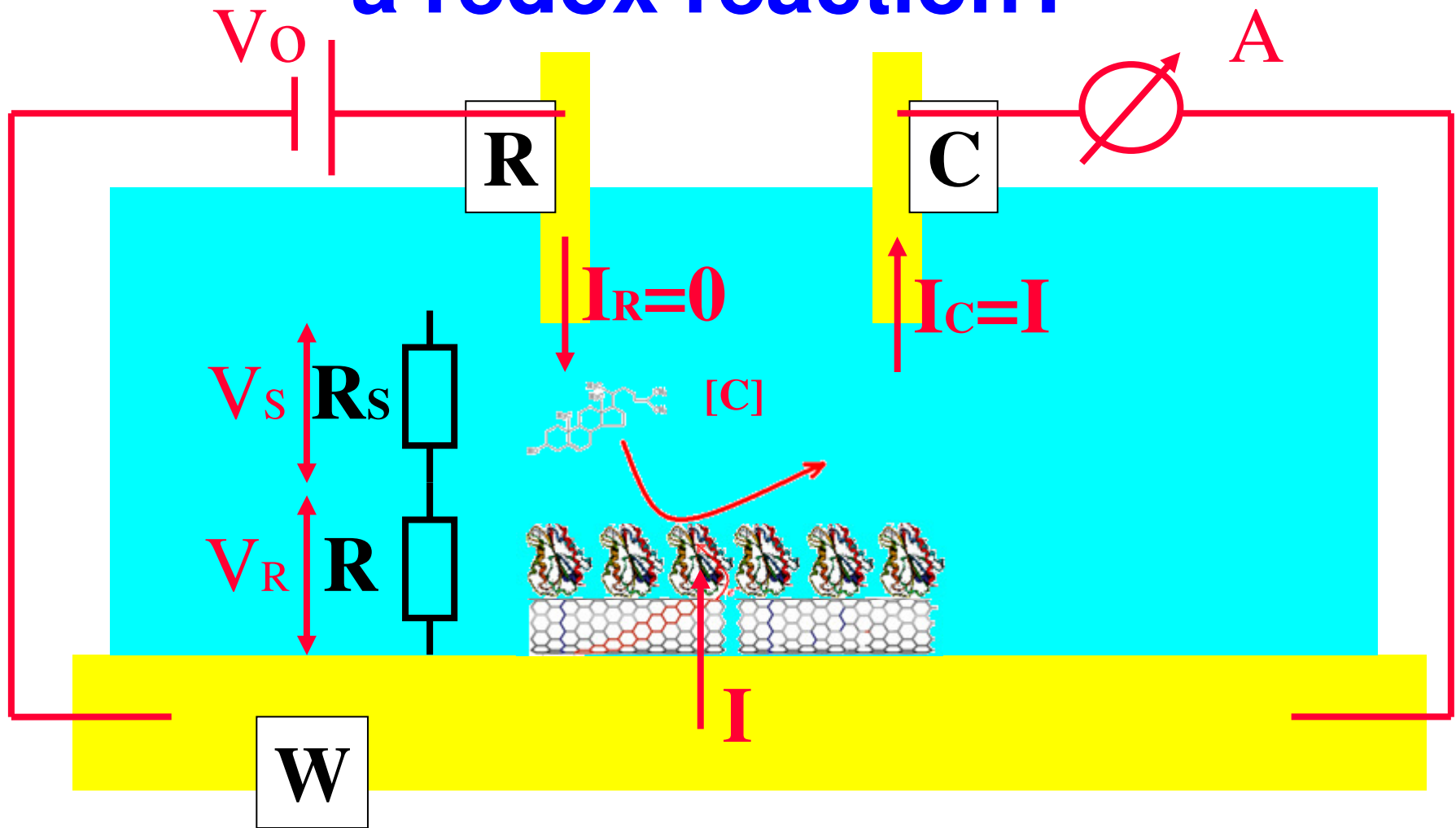


Working principle of Oxidases based detection

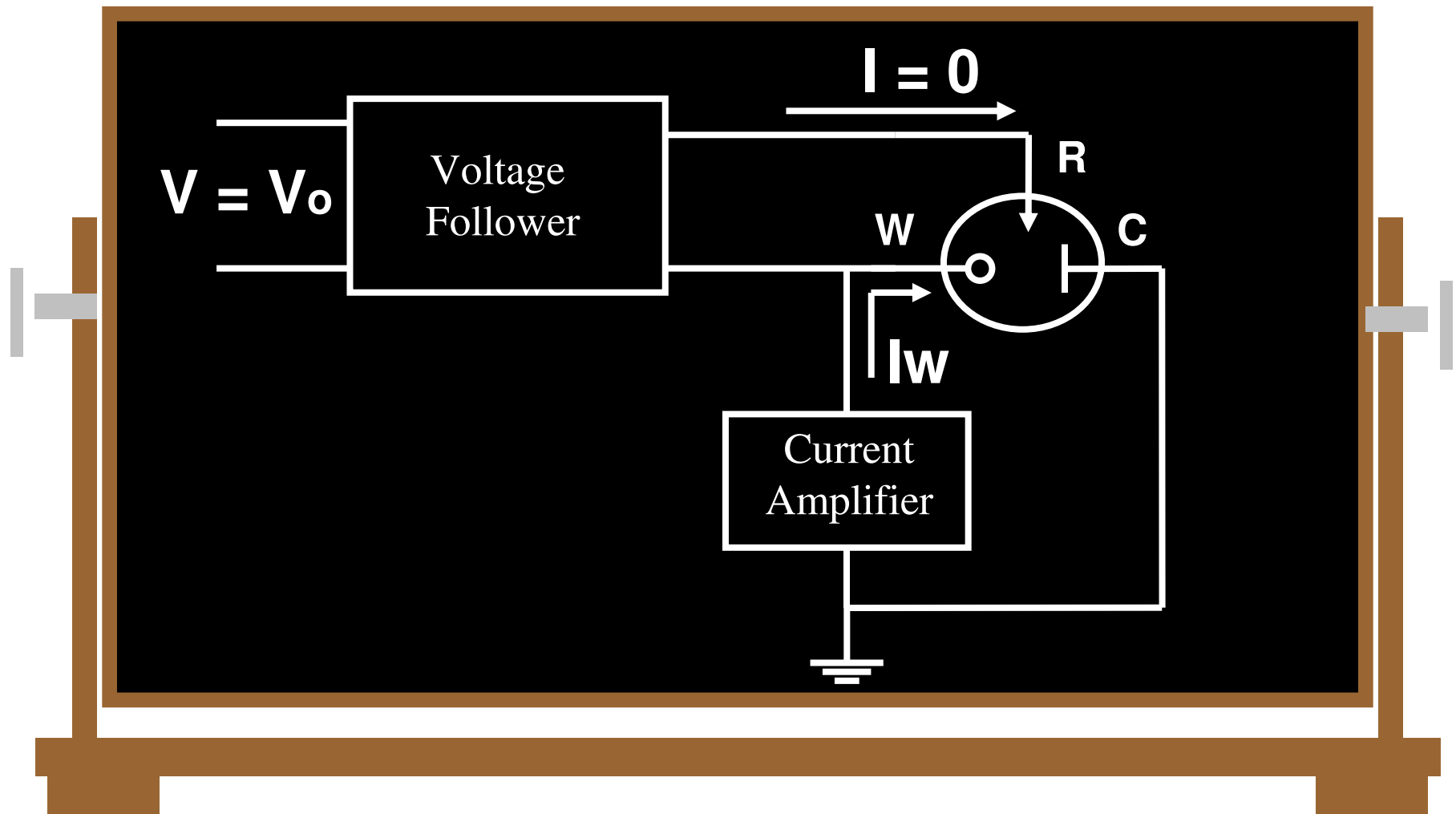


Amperometric
Detection !!!!!

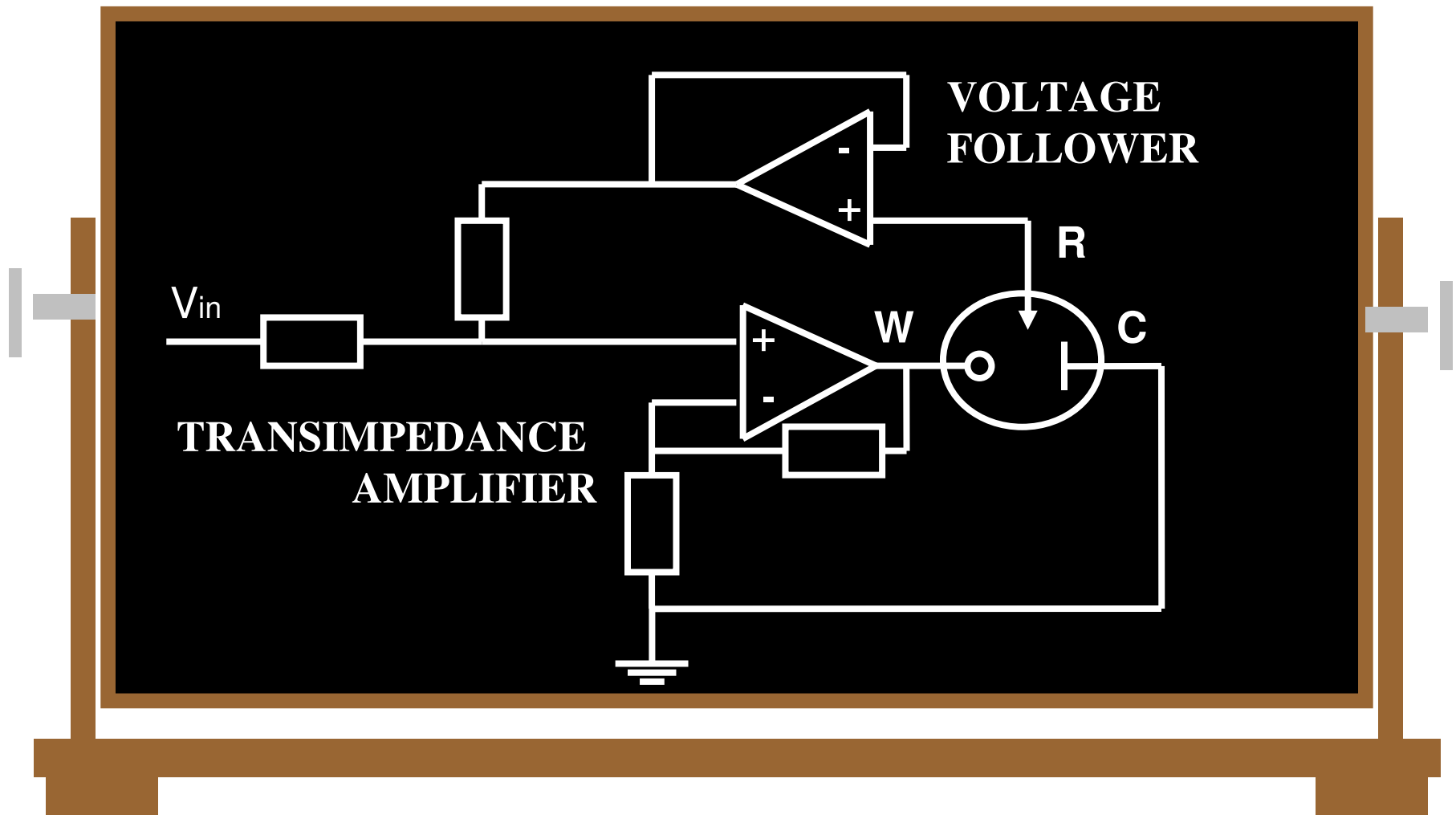
How to measure a redox reaction?



Required Blocks



The basic with Op. Amp.

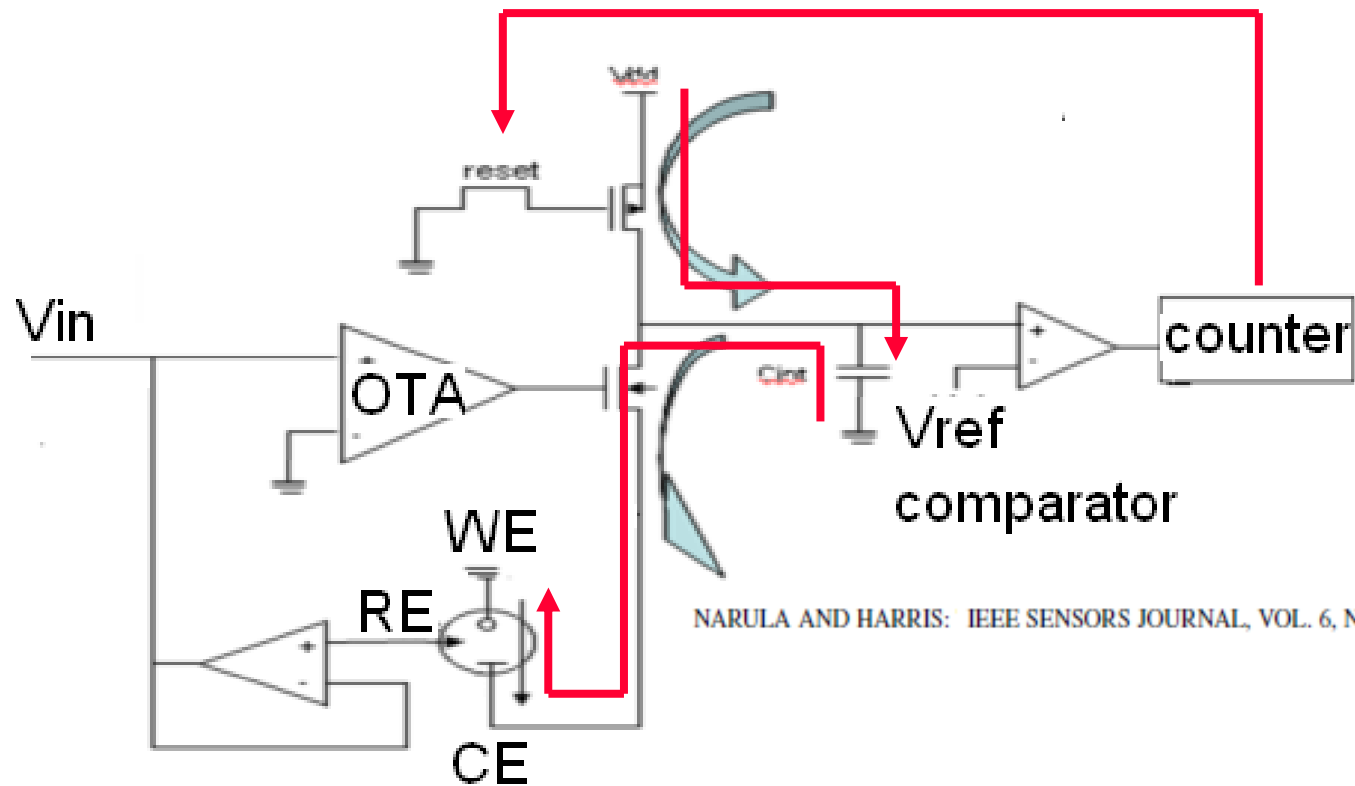


CMOS front-end demands

1. Precise Current measurements
2. Multiplexing for different molecules
3. Reliability in Temperature
4. Reliability in pH
5. Multiplexing Molecular Detection with T and pH

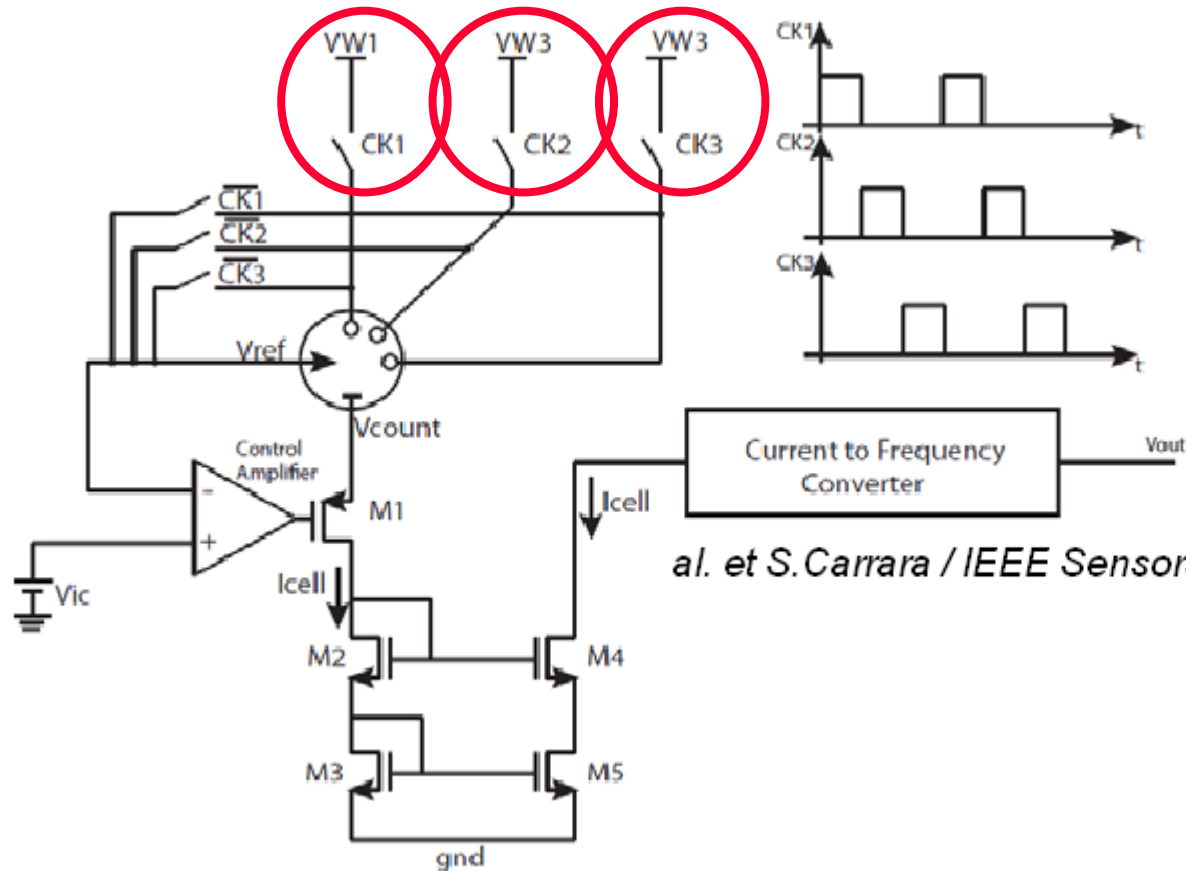
1. Precise Current measurements

Time Based Potentiostat



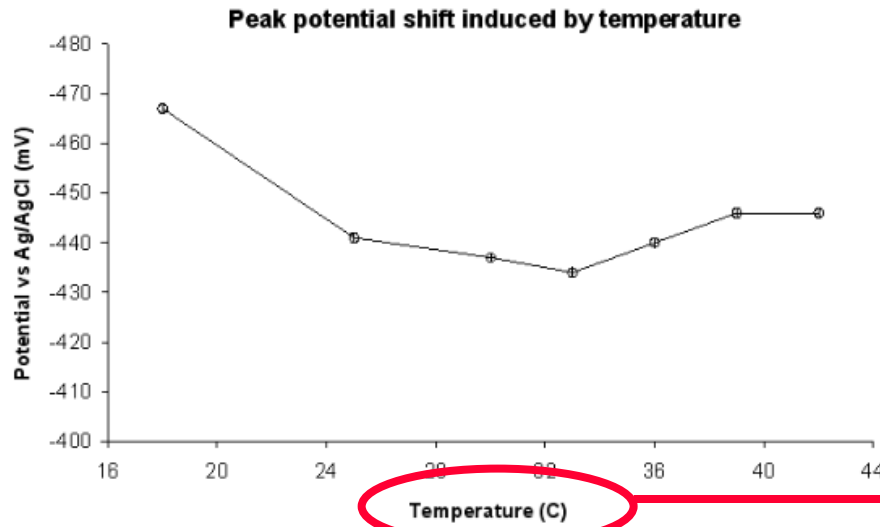
Current-to-frequency converter

2. Multiplexing for different molecules



Different working electrodes are multiplexed to the current-to-frequency converter

3. Reliability in Temperature

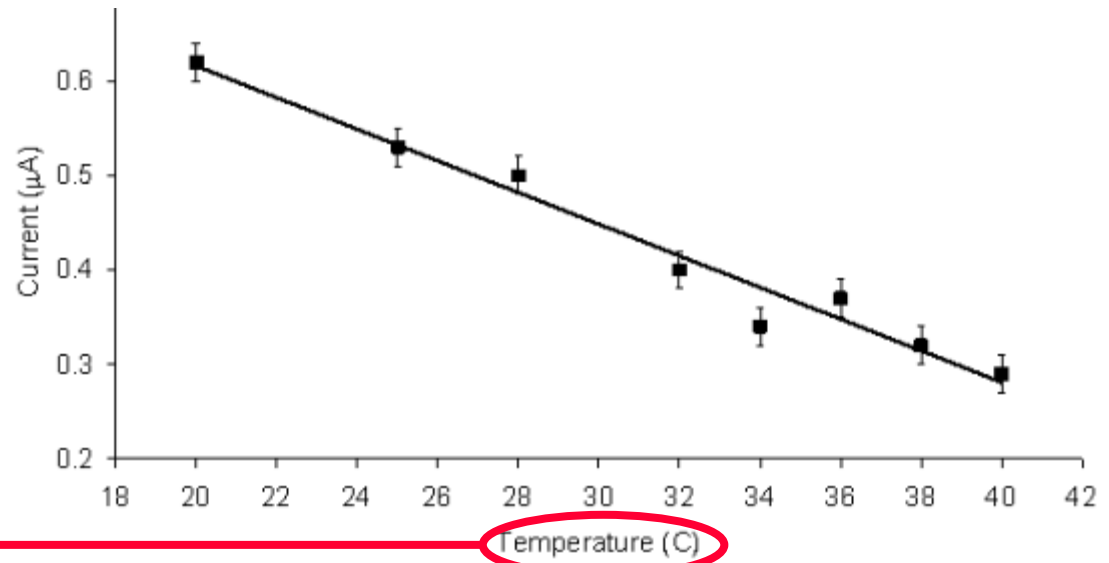


$$E = E^0 - \frac{RT}{nF} \ln\left(\frac{C_r}{C_o}\right) - \frac{RT}{F} pH$$

current variation induced by temperature

Figure 3. Peak Potential shift versus Temperature

$$i \propto nFAD \left(\frac{nFvD}{RT} \right)^{1/2} C_r$$



3. Reliability in Temperature

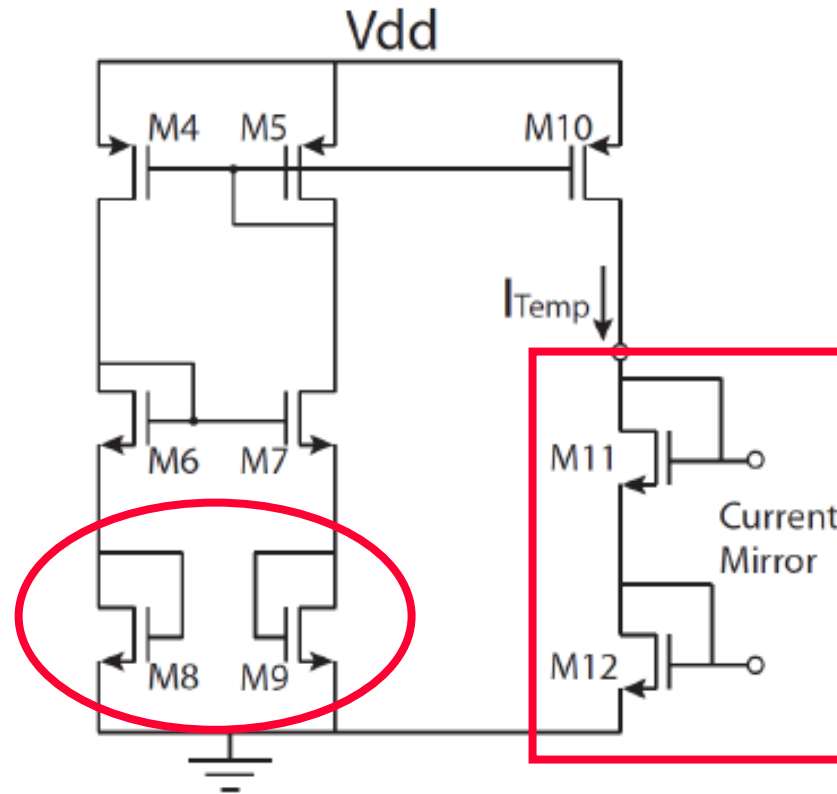
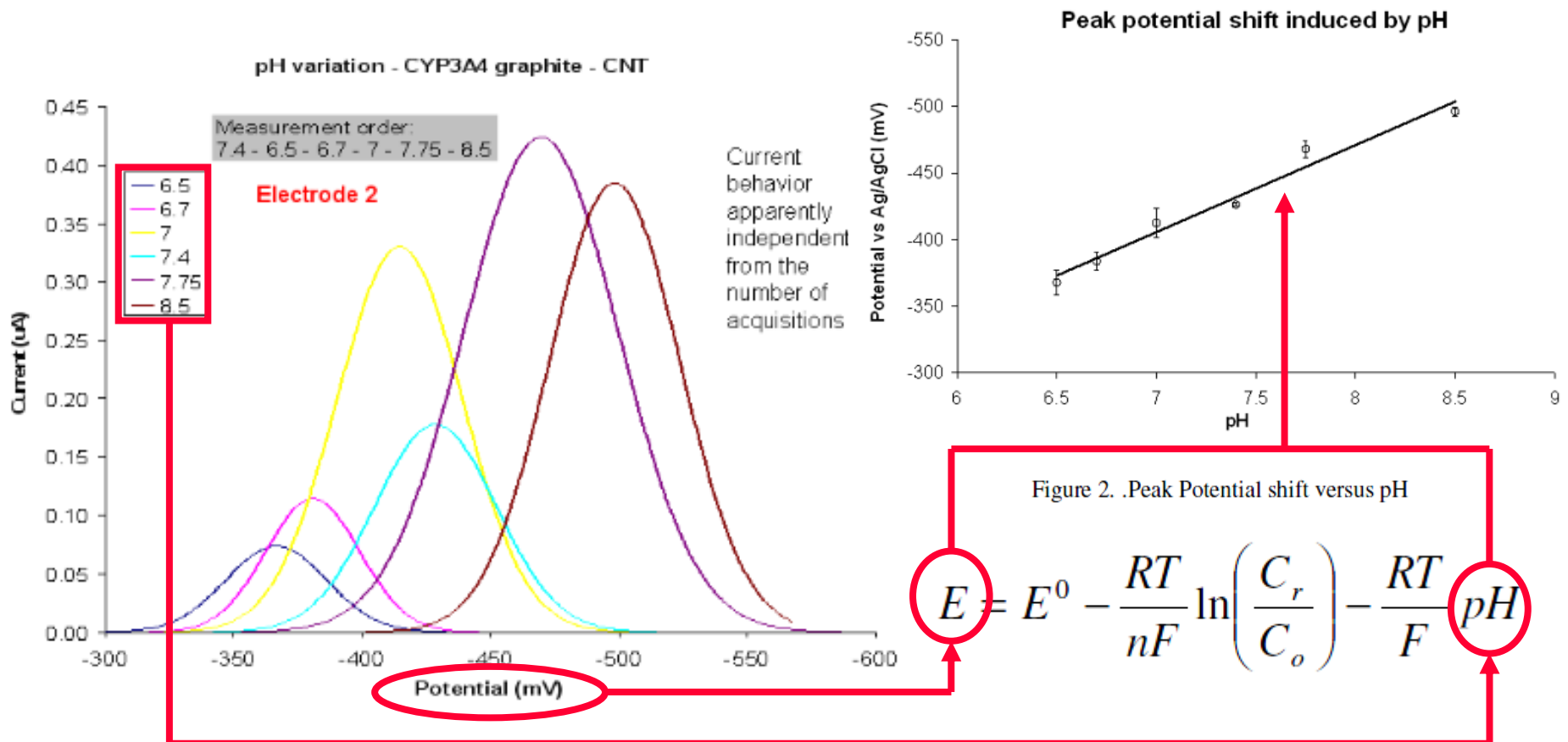


Figure 7. The circuit for the measure of Temperature

For VLSI, FET Transistor based circuits are more suitable than BJT

4. Reliability in pH



In CV, The peak position is pH dependant

4. Reliability in pH

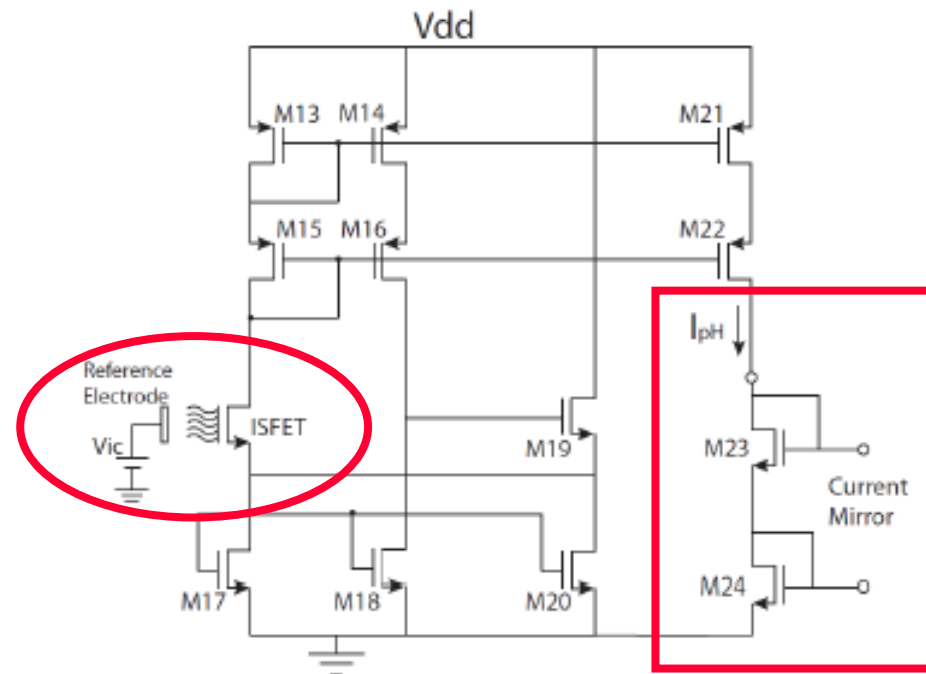
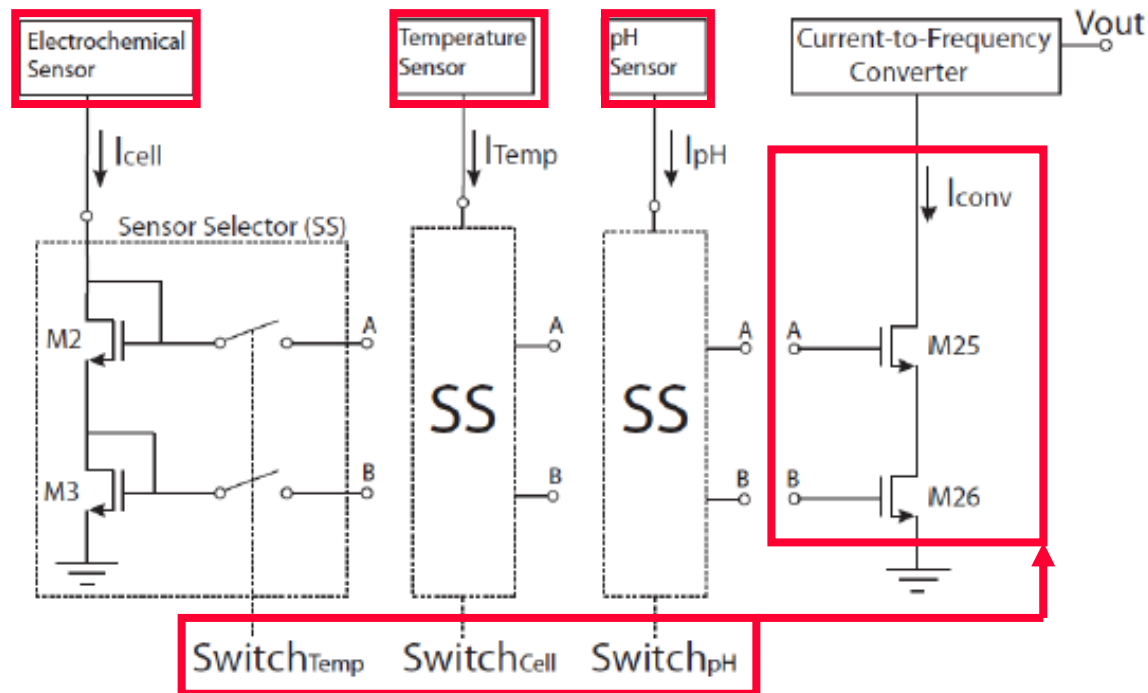


Figure 6. The ISFET sensors proposed by Premanode

The Ion-Sensitive FET measure the solution pH

5. Multiplexing Molecular detection with T and pH



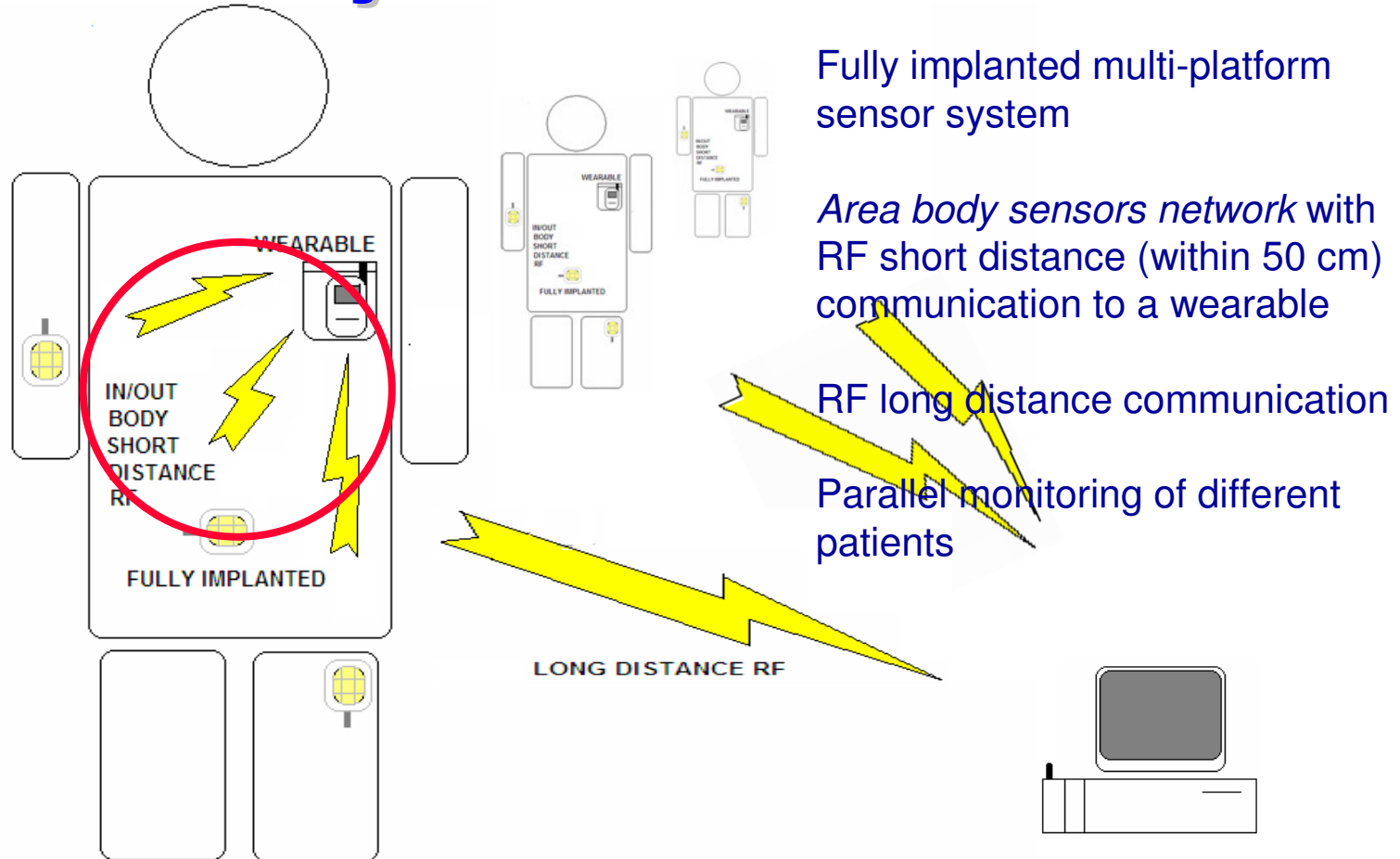
S. Carrara et al. / IEEE BioCAS 2010, submitted

Figure 8. The bloks-scheme of the multiplexing

The switches also multiplex the T and pH measure

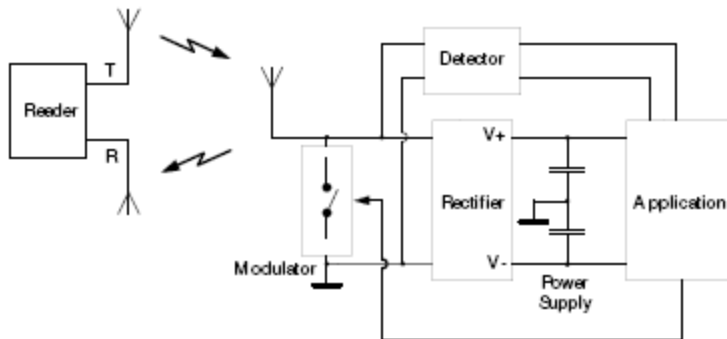


Project Main Goals



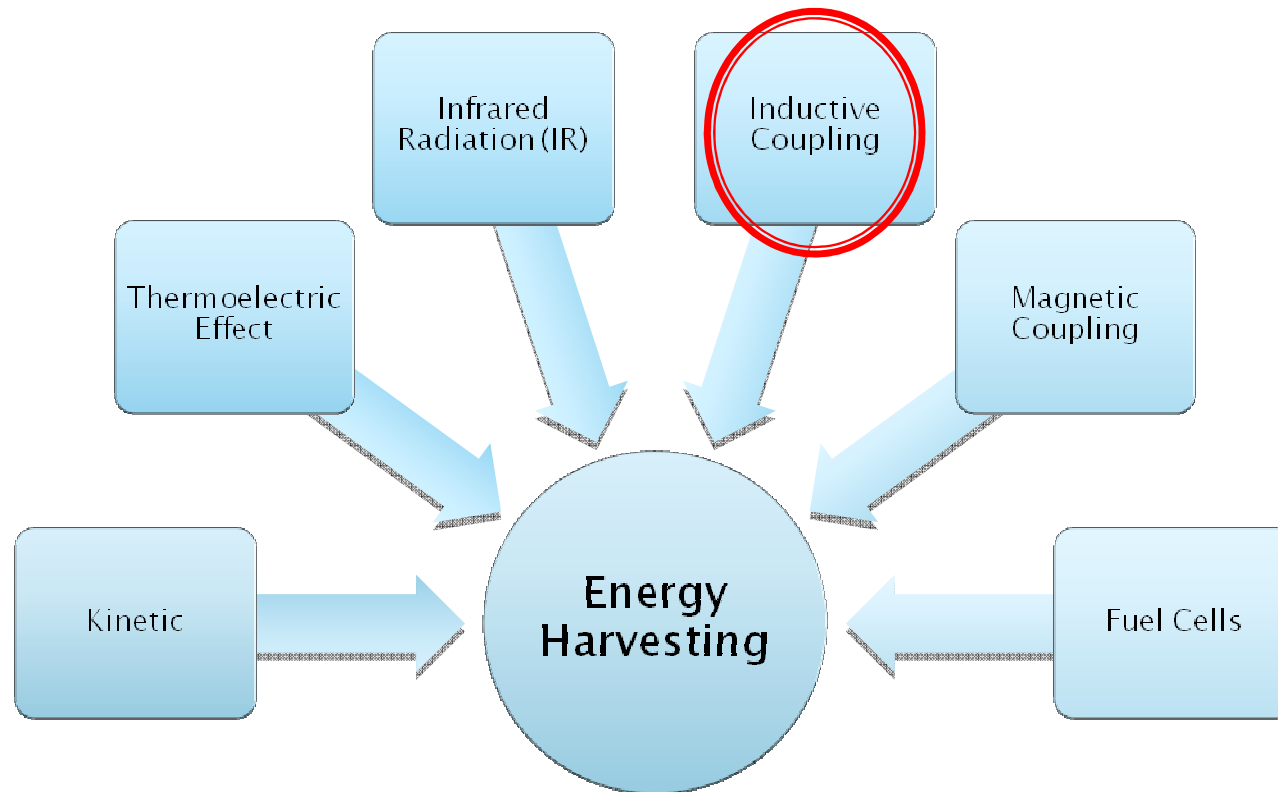
Design implantable/wearable systems for continuous monitoring of human metabolism

Data/power transmission



- The implanted sensors are remotely powered
- Bi-directional communication between external and internal units
- Ultra low power protocol and modulation
- Specific antenna design

Energy Scavenging Strategies

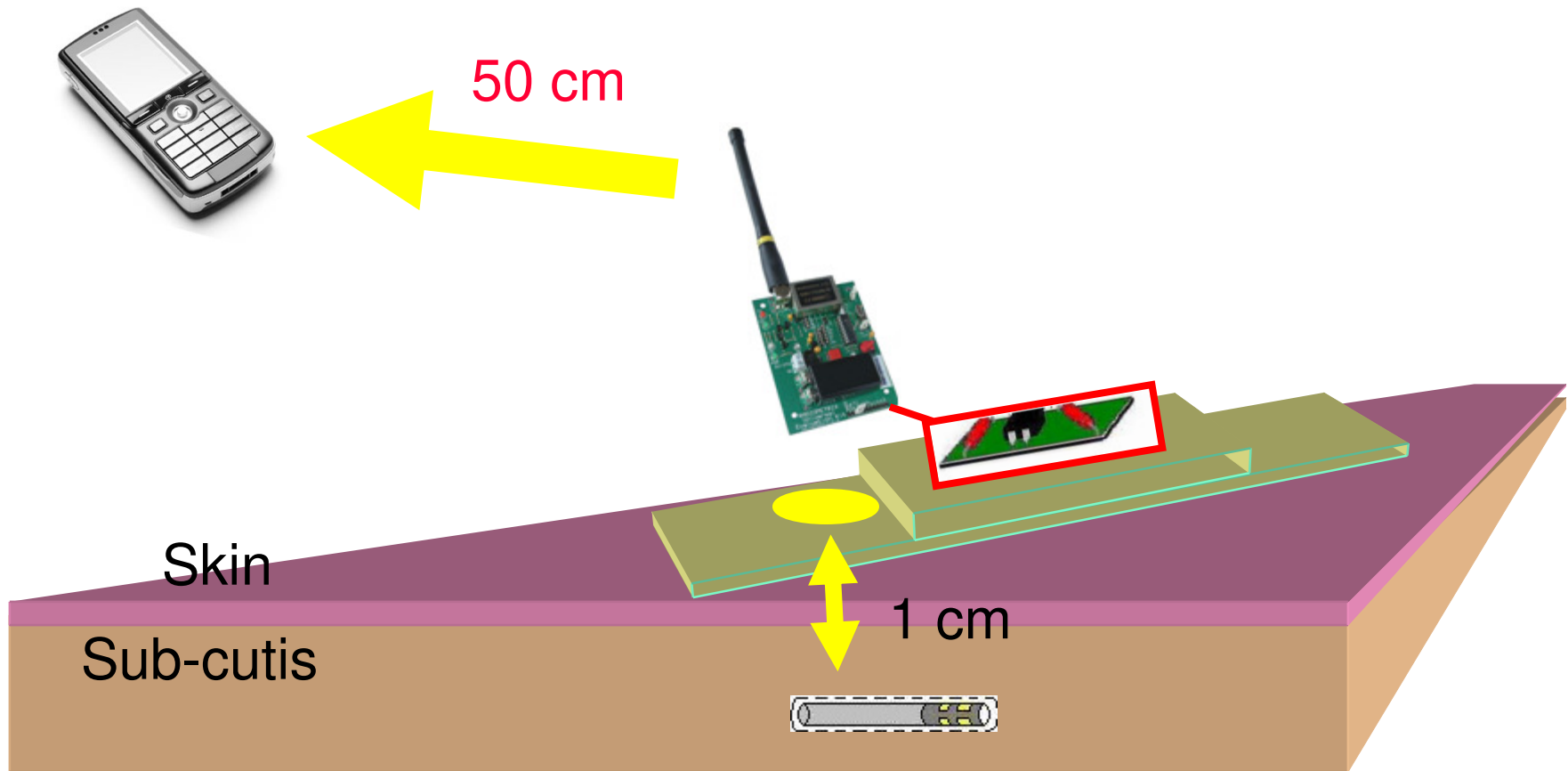


Inductive Coupling

Ref.	Coil Area ($\lambda = 10 \text{ mm}^2$)	Carrier Frequency	Data Transmission	Bit Rate	Power Consumption	Efficiency	Distance	Measurement Site	Implantation Site
[8]	Tx: 7.8λ Rx: 1.7λ	4 MHz	twd Int.: PWM-ASK twd Ext.: ASK	twd Ext.: 125 kbps	10 mW		5 mm	Air	Neural Recording System
[9]	Tx: 196.3λ Rx: 31.4λ	4 MHz	twd Ext.: LSK	5 kbps	6 mW		25 mm	Water Bearing Colloids	Various
[10]	Tx: 13200λ Rx: 25.2λ	1 MHz			150 mW	1% (min)	205 mm	PVC Barrel	Stomach
[11]	Tx: 184.9λ Rx: 10λ	1 MHz			10 mW	18.9% (max)	5 mm	Air	Cerebral Cortex
[12]	Tx: 282.7λ Rx: 31.4λ	0.7 MHz	twd Int.: ASK twd Ext.: LSK	twd Int.: 60 kbps twd Ext.: 60 kbps	50 mW	36% (max)	30 mm		Orthopaedic Implant
[13]	Tx: 31.4λ Rx: 5λ	10 MHz	twd Int.: ASK twd Ext.: BPSK	twd Int.: 120 kbps twd Ext.: 234 kbps	22.5 mW in vitro \approx 19 mW in vivo		15 mm	Rabbit	Muscles
[14]	Tx: 196.3λ Rx: 3.5λ	5 MHz	twd Int.: OOK	100 kbps	5 mW		40 mm		Neural Stimulator
[15]	\approx Rx: 112.5λ	6.78 MHz	twd Int.: OOK twd Ext.: LSK	twd Ext.: 200 kbps	120 mW	20% (max)	25 mm	Dog Shoulder	Muscular Stimulator
[18]	Tx: 40λ Rx: 0.4λ	915 MHz			0.14 mW	0.06%	15 mm	Bovine Muscle	Various

- [8] T. Akin et al., "A wireless implantable multichannel digital neural recording system for a micromachined shank electrode", *IEEE J. Solid-State Circ.*, vol. 33, pp. 109-118, Jan. 1998
- [9] C. Sauer et al., "Power Harvesting and Telemetry in CMOS for Implanted Devices", *IEEE Trans. on Circuits and Systems*, vol. 52, n. 12, pp. 2605-2618, 2005
- [10] B. Lanza et al., "An Inductive power link for a wireless endoscope", *Sensors and Biotechnology*, vol. 22, pp. 1890-1895, 2007
- [11] K.M. Sliay et al., "Load Optimization of an Inductive Power Link for Remote Powering of Biomedical Implants", *IEEE Proc. of International Symposium on Circuits and Systems 2009*, pp. 588-586, May 2009.
- [12] B. Lanza et al., "An Inductive power system with integrated bi-directional data-transmission", *Sensors and Actuators A*, vol. 115, pp. 221-229, 2004
- [13] J. Parramon et al., "ASIC-based battery less implantable telemetry microsystem for recording purposes", *Eng. In Med. and Bio. Soc.*, In *Proc. of the 19th Annual Int. Conf.*, vol. 5, pp. 2225-2228, 1997.
- [14] G. Gudrason et al., "A Chip for an Implantable Neural Stimulator", *Analog Integrated Circuits and Signal Processing*, vol. 22, pp. 81-89, 1999
- [15] B. Smith et al., "An externally powered, multichannel, implantable stimulator-telemeter for control of paralyzed muscle", *IEEE Trans. on Biomed. Eng.*, vol. 45, pp. 468-475, 1998
- [18] A.S.Y. Poon et al., "A mm-sized Implantable Power Receiver with Adaptive Link Compensation", Stanford University

Powering Patch



An antenna very close to the chip is required for the remote powering

Multiple Subcutaneous Sensor nodes



Different nodes in RF communication with a wireless portable devices

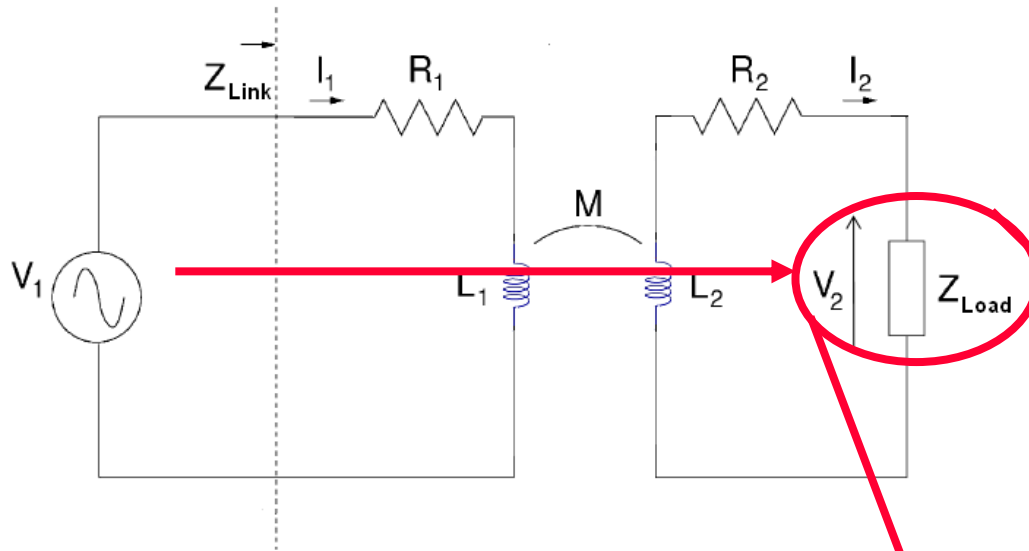
Inductive Coupling

Faraday Law: *The induced electromotive force in any closed circuit is equal to the time rate of change of the magnetic flux through the circuit.*

$$|\mathcal{E}| = \left| \frac{d\Phi_B}{dt} \right|$$



Inductive Coupling



$$|\mathcal{E}| = \left| \frac{d\Phi_B}{dt} \right|$$

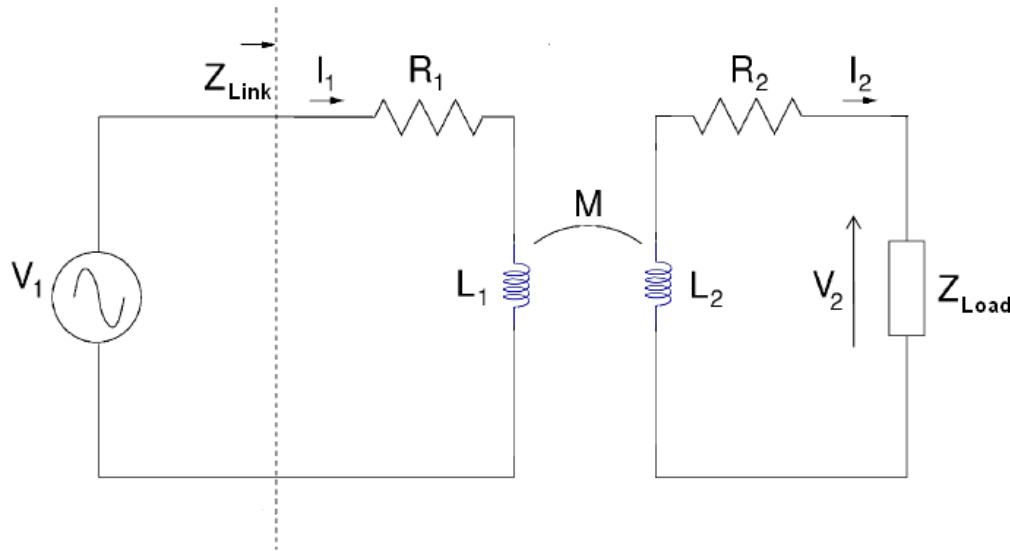
$$\begin{cases} L_1 = \frac{d\phi_1}{dI_1} \\ L_2 = \frac{d\phi_2}{dI_2} \\ M = \frac{d\phi_1}{dI_2} = \frac{d\phi_2}{dI_1} \end{cases}$$

$$\begin{cases} V_1 = +R_1 I_1 + \frac{d\phi_1}{dt} = +R_1 I_1 + L_1 \frac{dI_1}{dt} - M \frac{dI_2}{dt} \\ V_2 = -R_2 I_2 - \frac{d\phi_2}{dt} = -R_2 I_2 - L_2 \frac{dI_2}{dt} + M \frac{dI_1}{dt} \end{cases}$$



$$\begin{cases} V_1 = +R_1 I_1 + j\omega L_1 I_1 - j\omega M I_2 \\ V_2 = -R_2 I_2 - j\omega L_2 I_2 + j\omega M I_1 \end{cases}$$

Inductive Coupling



$$|\mathcal{E}| = \left| \frac{d\Phi_B}{dt} \right|$$

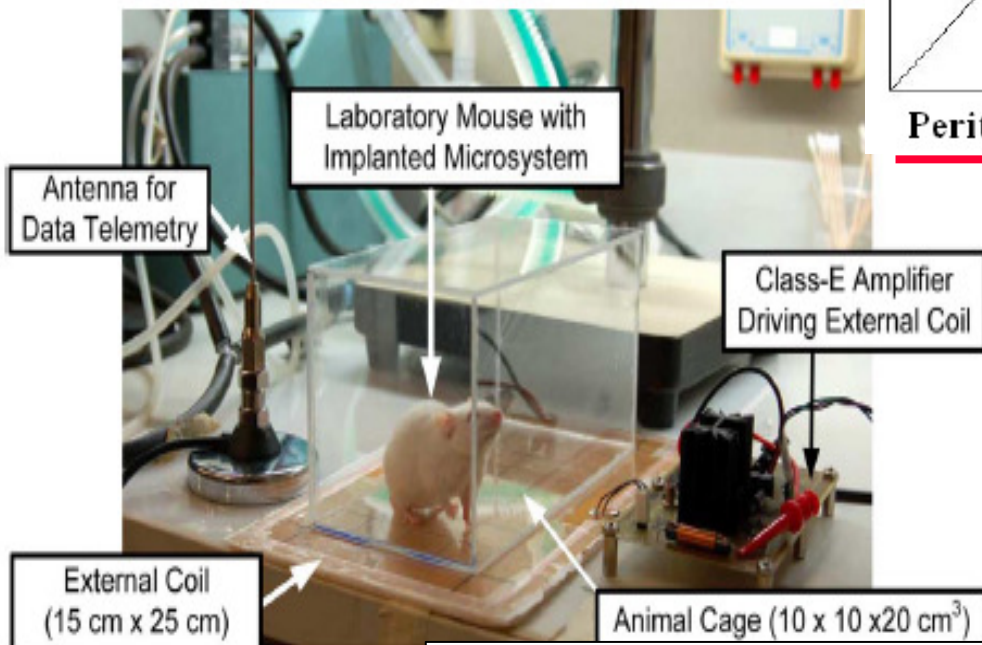
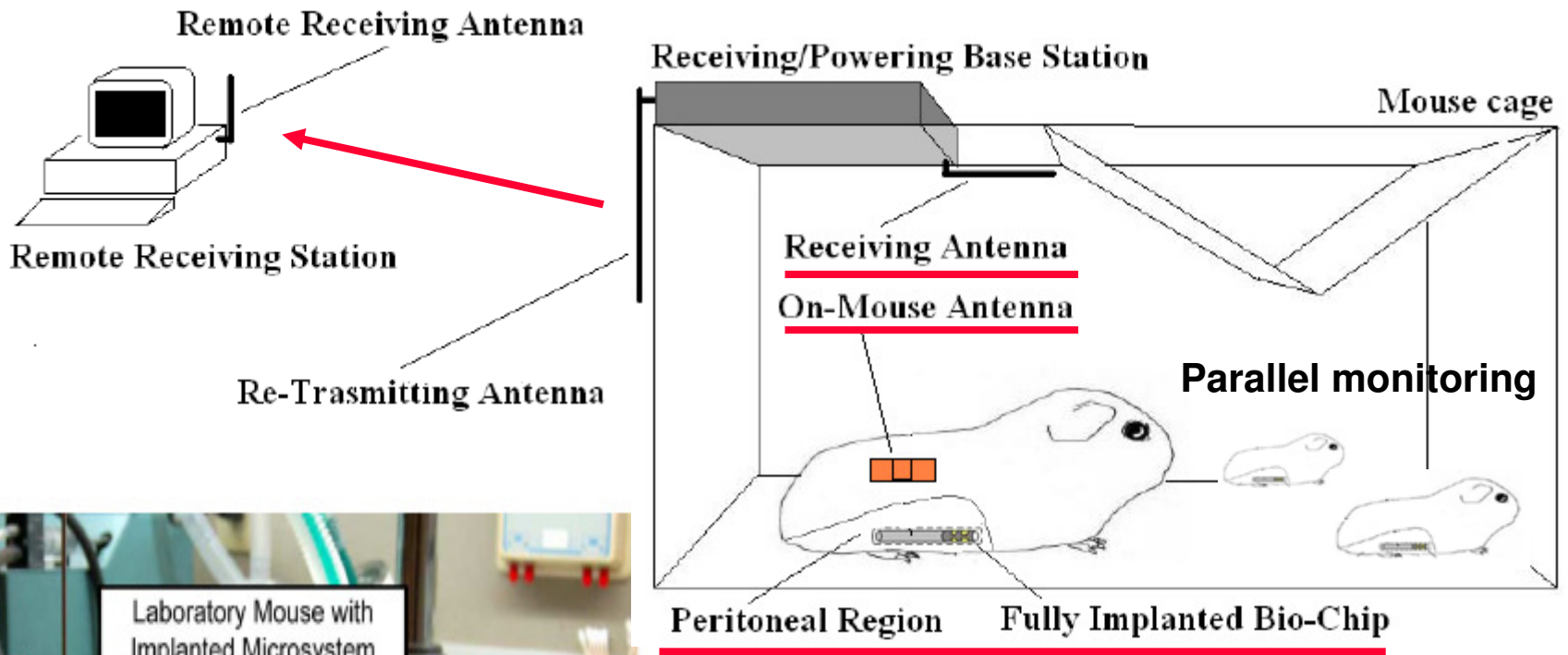
$$\begin{cases} L_1 = \frac{d\phi_1}{dI_1} \\ L_2 = \frac{d\phi_2}{dI_2} \\ M = \frac{d\phi_1}{dI_2} = \frac{d\phi_2}{dI_1} \end{cases}$$

$$V_2 = \frac{j\omega M Z_{Load}}{\omega^2 (M^2 - L_1 L_2) + j\omega (L_1 R_2 + L_2 R_1 + L_1 Z_{load}) + R_1 R_2 + R_1 Z_{Load}} V_1$$

$$\eta_{Link} = \frac{R \{V_2 I_2^*\}}{R \{V_1 I_1^*\}} = \frac{\omega^2 M^2 R_{Load}}{R_1 [(R_2 + R_{Load})^2 + (\omega L_2 + X_{Load})^2] + \omega^2 M^2 (R_2 + R_{Load})}$$

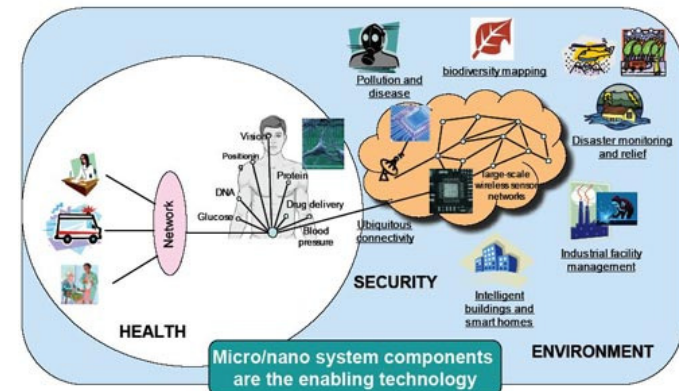
$$Z_{Link} = j\omega L_1 + R_1 + \frac{\omega^2 M^2}{j\omega L_2 + R_2 + Z_{Load}}$$

Test with animal models



Positioning within Nano-Tera.ch

- Large-scale data acquisition system:
Real-time data provided by nano-sensors
- Synergy:
Sensors, electronics, MEMS fluidics, data processing and communication
- Collaborative effort:
EPFL, ETHZ, EMPA, IRB
- Industrial participation:
Menarini, Nestle, ACS
- Social relevance:
Low cost and more accurate health monitoring



Implantable-IRONIC

Summary

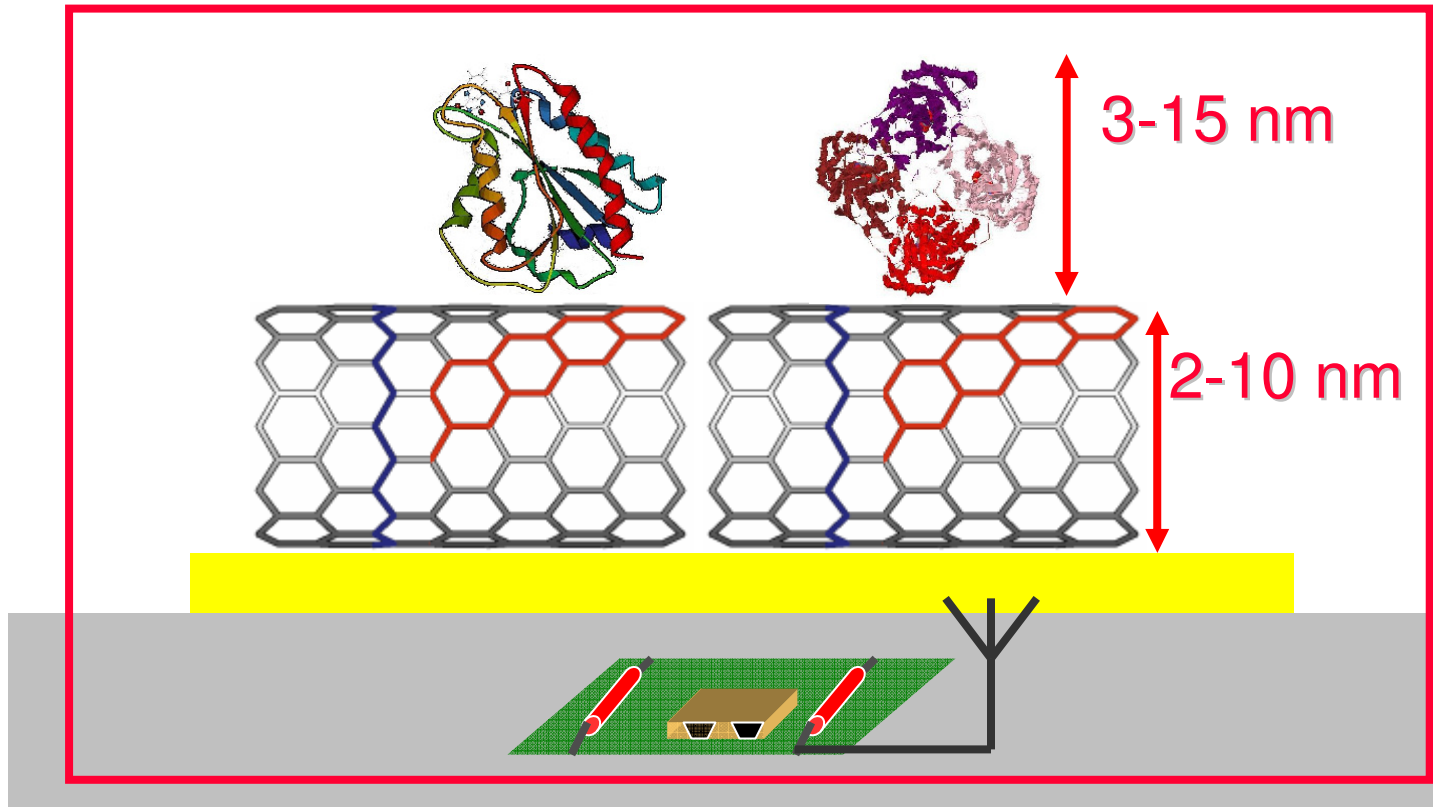
- Implantable/wearable system for *health monitoring*
With applications also to *personal nutrition*
- Flexible and *programmable* platform
 - New array-based *nano-structured* sensors
 - New low-power electronics for data acquisition and transmission
 - New real-time algorithms for data clustering
- Design, fabrication and test of demonstrators
 - Exploit FDA-approved implantable device by Menarini
 - Roadmap for realization and test in mice

Sensor/electronic/software co-design

- Sensors require specialized low-current detectors
 - Sensors designed to operate at low-voltage
 - Low-power sensor/electronic co-design
- Arrays yield multiple measurements
 - Different target molecules to be simultaneously detected
 - Redundancy is used to enhance dependability
- Data sampling and reduction before transmission
 - Low-effort *in situ* data processing
- Off-line algorithms for data disambiguation
 - Avoid false positives
 - Cluster data to provide signature for diagnosis

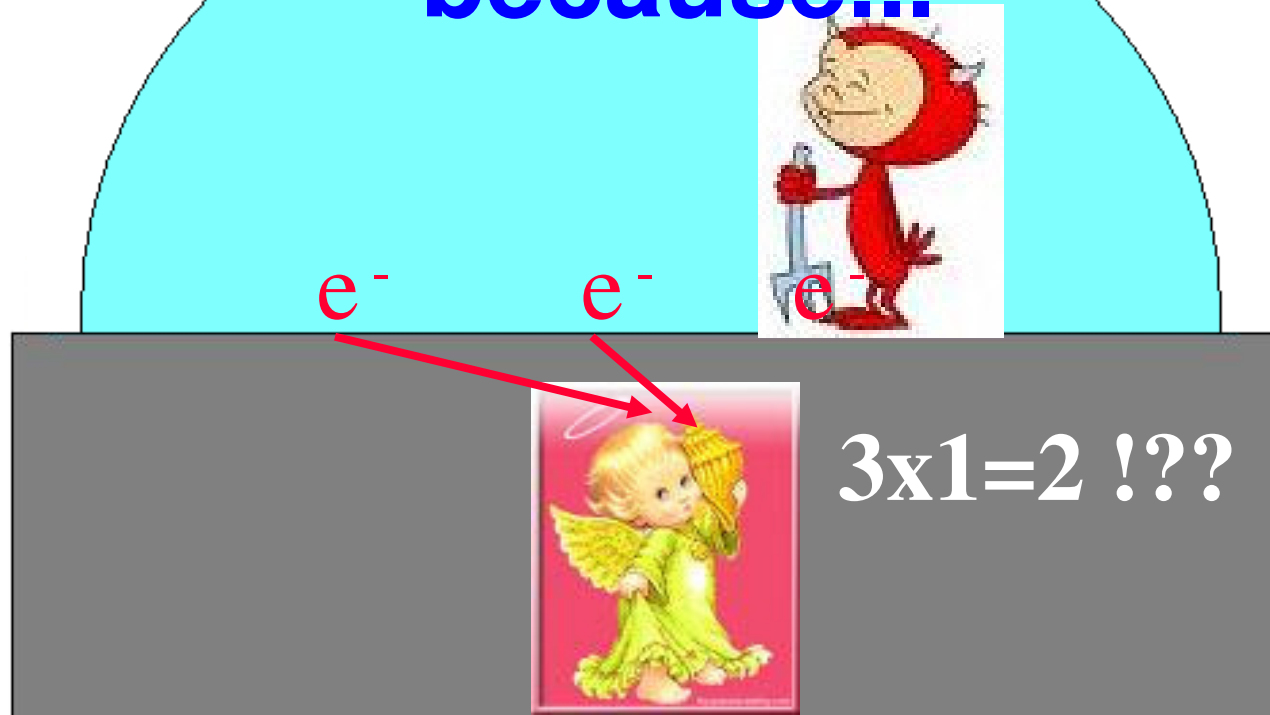
Conclusions

Nano/Bio/CMOS Co-Design!



New paradigms for Nano-Bio-CMOS co-design are required to succeed in distributed diagnostics

**New Paradigms are required
because...**



**Excellent CMOS technology is not sufficient
if molecules are not doing their own job at
the Bio/CMOS interface!**

Thanks to the Partners

SW & system integration: De Micheli

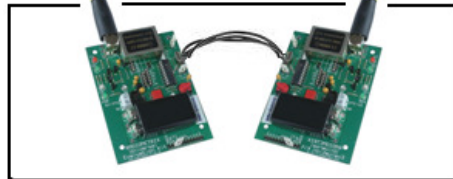


patient samples: F. Valgimigli



animal models: Grassi

Dehollain

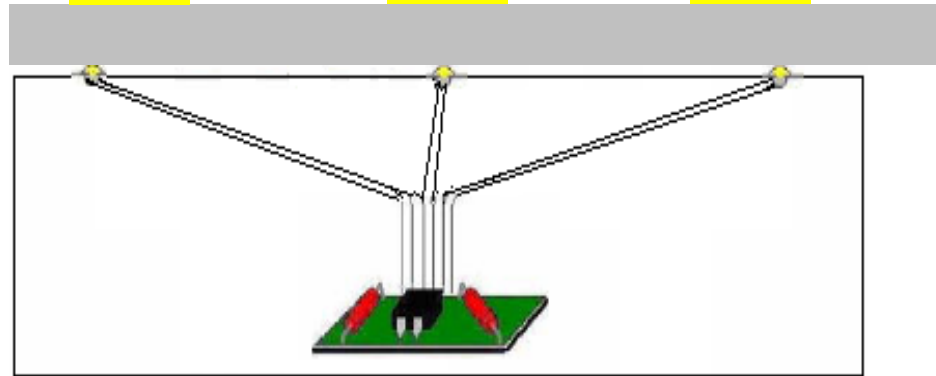


Huang
ACS

ACP AG
Advanced Circuit Pursuit

Thoeny

Carrara



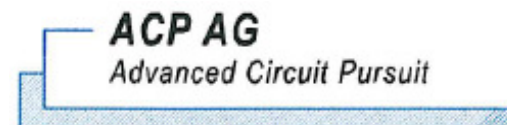
Leblebici



Personal nutrition: S. Rezzi

Partners contribution in terms of project technologies

Thanks to the Sponsors

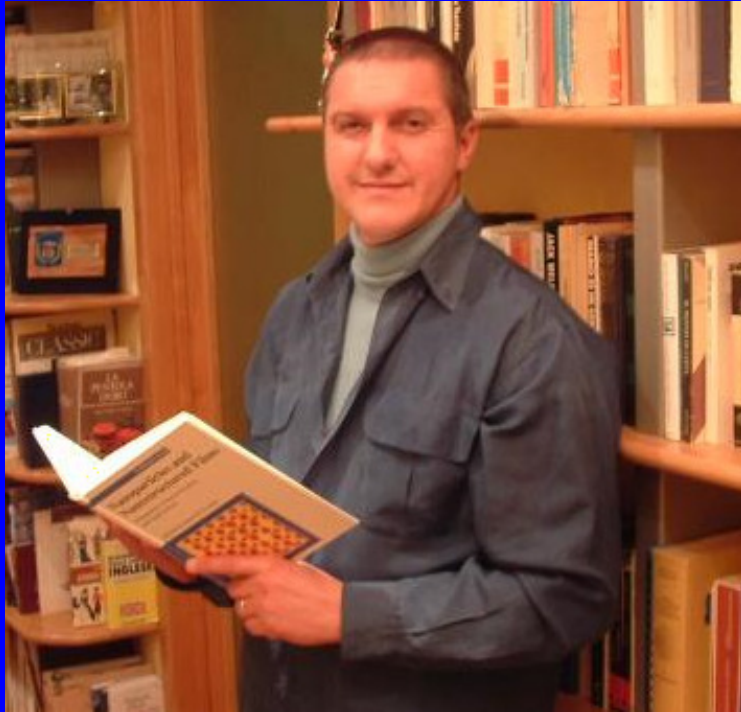


Thanks to my close collaborators

- *Andrea Cavallini*
- *Camilla Bai-Rossi*
- *Cristina Boero*
- *Jacopo Olivo*
- *Daniel Torre*
- *Daniela De Venuto*
- *Irene Taurino*
- *Alberto Tagliafierro*
- *Victor Erokhin*
- *Giovanni De Micheli*



Thank you for your attention!



Sandro Carrara Ph.D
EPFL - Swiss Federal Institute of Technology
in Lausanne - Switzerland

Web: <http://si2.epfl.ch/~scarrara/>
email: sandro.carrara@epfl.ch

References on biosensors:

1. Proceedings of IEEE/Bio-CAS 2010, submitted
2. Biosensors and Bioelectronics, (2010) submitted
3. Proceedings of the IEEE/ICME 2009, accepted
4. Biosensors and Bioelectronics, 24(2008) 148-150
5. Proceedings of IEEE/Bio-CAS 2008
6. Biosensors & Bioelectronics, 21 (2005) 217-222
7. Biosensor & Bioelectronics, 19 (2004) 971-976